I. ELECTRONIC PROCESSES IN α-SULFUR

II. POLARON MOTION IN A D.C. ELECTRIC FIELD

Thesis by

Karvel Kuhn Thornber

In Partial Fulfillment of the Requirements

For the Degree of

Doctor of Philosophy

California Institute of Technology

Pasadena, California

1966

(Submitted May 4, 1966)

ACKNOWLEDGMENTS

May I express my sincerest gratitude to Professor Carver A. Mead for his never ceasing guidance and support throughout the two projects reported here and in many others as my advisor. To Professor Richard P. Feynman, in whose mind the solution to the Polaron problem was conceived, may I extend my sincerest thank you for patiently guiding me through the problem, pointing out so many relevant ideas and general methods in its course. May I thank also Mr. H. M. Simpson for technical help in the Sulfur experiment and Dr. Robert V. Langmuir for financing the time-consuming computer work in connection with the Polaron. To Mr. Thomas C. McGill I acknowledge help with the basic computer program. Many thanks also to the National Science Foundation for a Cooperative Graduate Fellowship, and to the Office of Naval Research and ITT for partial support of the research.

ABSTRACT

Part I: The mobilities of photo-generated electrons and holes in orthorhombic sulfur are determined by drift mobility techniques. At room temperature electron mobilities between 0.4 cm^2/V-sec and 4.8 cm^2/V-sec and hole mobilities of about 5.0 cm^2/V-sec are reported. The temperature dependence of the electron mobility is attributed to a level of traps whose effective depth is about 0.12 eV. This value is further supported by both the voltage dependence of the space-charge-limited, D.C. photocurrents and the photocurrent versus photon energy measurements.

As the field is increased from 10kV/cm to 30 kV/cm a second mechanism for electron transport becomes appreciable and eventually dominates. Evidence that this is due to impurity band conduction at an appreciably lower mobility ($4. 10^{-4}$ cm^2/V-sec) is presented. No low mobility hole current could be detected. When fields exceeding 30 kV/cm for electron transport and 35 kV/cm for hole transport are applied, avalanche phenomena are observed. The results obtained are consistent with recent energy gap studies in sulfur.

The theory of the transport of photo-generated carriers is modified to include the case of appreciable thermo-regeneration from the traps in one transit time.

Part II: An explicit formula for the electric field E necessary to accelerate an electron to a steady-state velocity v in a polarizable

crystal at arbitrary temperature is determined via two methods utilizing Feynman Path Integrals. No approximation is made regarding the magnitude of the velocity or the strength of the field. However, the actual electron-lattice Coulombic interaction is approximated by a distribution of harmonic oscillator potentials. One may be able to find the "best possible" distribution of oscillators using a variational principle, but we have not been able to find the expected criterion. However, our result is relatively insensitive to the actual distribution of oscillators used, and our E-v relationship exhibits the physical behavior expected for the polaron. Threshold fields for ejecting the electron for the polaron state are calculated for several substances using numerical results for a simple oscillator distribution.

CONTENTS

PART I

ELECTRONIC PROCESSES IN α-SULFUR

I. 1. Introduction

The recent determination of the band gap of α-sulfur from photo-response measurements at this laboratory[1] indicated that both holes and electrons should be mobile charge carriers. As a result of that investigation, the energy gap of orthorhombic sulfur was found to be 3.82 ± 0.02 eV from both electron and hole photocurrent. For hole current only, moreover, a distinct and ever-present local maximum was found between 0.44μ and 0.45μ (Fig. 1). This was attributed to the presence of a trapping level about 2.8 eV above the valence band to which electrons could be excited, freeing holes in the valence band for conduction. The rather gradual but steady decrease of the photocurrent for wave lengths beyond the band gap indicated that shallow defect levels might also be present. A typical series of measurements from this work is shown in Fig. 1.

The results of the work reported here substantiate these hypotheses and render additional insight into previous investigations. Although both hole and electron current were found present in comparable amounts, the emphasis is given to electron current: the corresponding determination and analysis of hole current in α-sulfur has already been ably presented by Adams and Spear.[2] Our investigations of the hole current agreed quite well with their work;

+ This work is published with Professor C.A. Mead, California Institute of Technology, in J. Phys. Chem. Solids, 26, 1489, (1965).

however, an equally strong case for electron current is also given. Several effects indicated in an earlier account[3] of electron charge transport under greatly restricted conditions are treated more thoroughly, the results of which yield a reasonably consistent picture of currents in the insulator sulfur.

I. 2. Specimen Preparation and Experimental Procedure

The samples were grown and prepared as before.[1] Grown from CS_2 solution at 15°C, they were lapped to 0.1-1 mm, and chemically polished in benzene. Consistent with the previous work, the response was essentially independent of the metal electrodes used. Semi-transparent gold dots were evaporated at 10^{-6} Torr to one side of the sample and a continuous layer applied to the opposite side. Great care was taken to prevent heat damage to the surfaces. In some cases, to minimize this heat damage, no gold was evaporated on one side of the sample, but contact was made directly to a thin brass mounting plate with silver paste. The response did not differ appreciably from those made by the former method.

The sample is mounted in a shielded container, and contact to the gold dot is made with a 4 mil gold wire probe. About 10^9 electrons and holes are excited when the sample is illuminated by a light pulse from a "Fischer-Nanolite". The duration of the pulse is about 10 n sec, a time appreciably shorter than any other time of interest. Due to the high absorption coefficient[1] at wavelengths shorter than $\approx 0.325\mu$, the electron-hole pairs are created in a very thin layer (≈ 0.001 cm) near the illuminated surface of the sample. that most carriers are generated band to band is indicated by the

relative magnitude of the photocurrent at larger wavelengths. Depending on the polarity of the gold dot, either electrons or holes can be drawn across the bulk of the sample, and mobilities can be determined by the standard method.[4-7] (The charge transported versus time is observed with an oscilloscope; the variation of the transient time with applied field gives the mobility. Fig. 5.) It was never necessary to build up space charge in deep traps in order to observe carrier transport of either sign. Allowing such space charge to accumulate only reduced the magnitude of the transported charge by about 20% but did not appreciably alter the shape of the charge versus time characteristics. The magnitude of this space charge could be determined by illuminating the sample with no applied bias and observing the transport of carriers of the opposite sign. (Fig. 2). By comparing this result with that for the sample biased for the same carrier but with no space charge present, an expression for the field at the illuminated layer and hence the equivalent space charge field can be obtained. This space charge could be readily neutralized by illuminating the sample at zero bias several times until no charge transport could be observed. The neutralizing charge could recombine with the space charge or become trapped itself. Our results indicate that the latter mechanism might be the more likely one.

I. 3. Results

The results of the drift mobility measurements are summarized in Table 1. As mentioned before, hole transport is found to be in good agreement with the work of Adams and Spear,[2] and is not analyzed here. Indeed hole mobilities could have been measured

for all samples, as was done for electron mobilities. With one notable exception the electron mobilities at room temperature range from 0.40 to 4.8 $cm^2/V\text{-}sec$ comparable to hole mobility. For samples showing a low electron mobility, a very steep slope appeared during the first 50 n sec of the charge versus time characteristic. In magnitude this represented about 5 to 10% of the total charge transported (but remained constant with voltage for any one sample), and was attributed to holes being drawn into the illuminated electrode, as pointed out earlier by Spear.[4] Note that this is just the contribution to charge transport expected from charge traversing only 5 to 10% of the sample.

Assuming a trap controlled drift mobility,[6-7] which implies

$$\mu_e = \mu_L \left(1 + N_t/N_c \cdot \exp(E_t/kT)\right)^{-1}, \qquad (1)$$

one may determine the effective trapping level E_t for electrons below the conduction band, and the density of trapping centers N_t. Assuming the variation of lattice mobility with the temperature to have the form $\mu_L = LT^{-3/2}$, μ_L may also be determined. The temperature of the sample was varied from 0^oC to 90^oC: E_t was found to be 0.12 ± 0.01 eV and N_t of the order of $2.8 - 3.5 \times 10^{17}\ cm^{-3}$. A room temperature "lattice mobility" of about $2\ cm^2/V\text{-}sec$ is indicated. Carrier transport in sample E appeared to be dominated by "lattice" interactions over the temperature range investigated. (While the source of the variation of "lattice" mobility from sample to sample was not investigated, that such a variation

exists is certainly not unexpected.)

The trapping level and densities reported above are stated as "effective" or "equivalent" values. The nature of the photo-response versus wavelength for wavelengths beyond the energy gap can be explained by assuming that distributions of hole and electron traps exist in the band gap which decay more or less exponentially away from the respective band edges. According to Rose,[8] under these conditions the d.c. photocurrent versus applied voltage for a fixed excitation rate should vary as

$$I \propto V^{(T_c/T + 1)}, \tag{2}$$

where kT_c is the effective trapping level, and is related to the trap density per unit energy by

$$N_t(E) = A e^{-E/kT_c} \tag{3}$$

where E is the energy between the band edge and the trapping level. Such measurements for electron photocurrent gave an effective level of 0.13 eV, in good agreement with that obtained from thermal measurements. (Fig. 3). For hole current an effective level of 0.18 eV was calculated, in good agreement with the 0.19 eV found by Adams and Spear.[2] Finally, a careful analysis of the variation of photocurrent with wavelength (Fig. 1) just beyond the band edge (0.325μ) gives an effective level of 0.11 eV for electron traps and 0.21 eV for hole traps. This third determination of the trapping levels is most reassuring. Analyzing this photo-response for longer wavelengths suggests the existence of other hole and electron traps whose density is also exponential in energy, and whose characteristic kT_c values are 0.4

to 0.7 eV. The cross section of these traps seems to be sufficiently low that they do not affect the currents measured here.

The last column of Table 1 records the room temperature mobilities for electrons transported across the sample at about one-ten-thousandth the rate of the electron transport described above. These negative charge carriers appear as a small additional contribution to the first electrons at 10 kV/cm, but by 40 kV/cm this current is so large as to completely dominate the characteristic, except for times less than about 10 μ sec. (Figs. 3-5). Above 30 kV/cm, another effect enters which contributes to this secondary charge transport (described below). Between 10 kV/cm and 30 kV/cm, the authors attribute the source of this low mobility electron current to be conduction via the previously reported[1] impurity band of electron traps located at about 2.8 eV about the valence band (1.0 eV below the conduction band).[10] Further association of currents with this band is discussed below as well as a third determination of this energy level. No corresponding low mobility hole transport could be detected.

I.4 The Avalanche Phenomena

To further analyze the low mobility electron current above, the circuitry was modified so that current versus time was observed instead of the usual charge-time characteristic. The results obtained for fields below 30 kV/cm are consistent with the above model: a short duration (50 μsec) of high mobility current is followed by a 400 μsec decay, and then a 500 to 3000 μsec of nearly constant mobility current about half the magnitude of that for the high mobility electrons. For hole current the decay from the quickly reached initial maximum to the zero level is much sharper, the time constant varying inversely with

applied field (8 μsec at 20 kV/cm), and no low mobility current plateau is detected.

The observations for both hole current above 35 kV/cm and electron current above 30 kV/ cm were indeed unexpected (Fig. 6). Illuminating the surface of the neutralized sample with the nanolite for either voltage polarity, current versus time characteristics of identical form to those described above would be obtained for times less than about 1 m sec for electrons and 0.1 m sec for holes. This expected behavior is then followed by a series of current spikes lasting for about 4 msec for electrons to 20 msec for holes. The decay times of these pulses were within 10% of the RC time constant (8 μsec) of the input circuit. The spikes were also about equally spaced in time (0.1 to 0.5 msec) over most of their duration, and after an initial rise, their amplitude decayed exponentially in time.

To investigate the source of this avalanching, light from a monochrometer was focused on the sample and the above measurements repeated, as the wavelength of monochrometer light was reduced from 3.0 μ. The spikes in the hole current could be suppressed only for frequencies near the energy gap (0.325μ, 3.82 eV). The electron current spikes, however, were repeatedly suppressed for photon energies of 0.96 eV. Neutralizing the sample and repeating the measurements, a somewhat higher photon energy was necessary to suppress the avalanche. The maximum equilibrium energy necessary after many runs was 1.10 eV.

These results are seen to be consistent with the energy gap data already obtained if viewed in the following manner. With no d.c. light source, the neutralized sample is illuminated as before, and hole

current is drawn through the material, some of it being trapped in the broad trapping levels noted earlier. This space charge enhances the field at the electrode opposite the illuminated one sufficient to cause the avalanche. With a d.c. illumination near the band gap, these traps may be emptied sufficiently rapidly that the space charge field required for avalanche cannot be established. That the avalanching carrier in fact ejects a hole from a trap as opposed to a band to band avalanche is evidenced by the fact that the spikes die off in time much faster than the thermal release time of the holes. Trap ejection reduces the space charge and hence the field causing avalanche. A similar argument can be given for electrons. However, owing to the predominate band of electron traps at 2.8 eV above the valence band, the effect is much better defined. Again, when the neutralized sample is illuminated with no d.c. light source, the low mobility electron current enhances the negative charge in this band which in turn increases the field at the unilluminated electrode. In such a field, carriers in the conduction band can avalanche with the trapped carriers and reduce the space charge below the critical level. When the same experiment is performed with d.c. illumination at 1.0 eV, these traps are emptied sufficiently rapidly while the high and low mobility currents are flowing that no avalanching can occur. Repeated neutralization of the crystal then increases the amount of positive charge in the hole traps needed to neutralize the slight increase in negative charge in the electron traps. With more holes in traps there would be a tendency for recombination in addition to trapping, both effects contributing to a larger space charge field which would have to be reduced to suppress the avalanche. And to remove more electrons from the traps a slightly higher photon

energy must be used. The limiting value for this is about 1.1 eV. The mechanism of the avalanche may well be similar to that discussed by Haitz.[11]

Dean et al.[3] reported seeing electron current pulses, which were attributed to field emission effects at the electrodes. That this was not the case here is easily seen by the fact that holes emitted from the collecting electrode would traverse the sample and relatively few would be trapped in the transit at such short transit times. Hence the avalanche would occur for a much longer duration than with the opposite bias. For this opposite bias (the illuminated electrode positive so that holes initially traverse the sample), under the field emission hypothesis, electrons would be forced into the sample by the emission, and the hole space charge would be neutralized more quickly. In fact the opposite was the case. Avalanche attributed here to holes near the collecting electrode was two to ten times longer lived than the corresponding electron avalanche. Hence field emission, if present, plays only a minor role compared to the avalanche of carriers from traps.

I. 5. Supplemental Support of Findings*

Shortly after the preceding four sections appeared in print, we were challenged to demonstrate that the fast electron current we had discovered was in fact not due to holes drifting the other way and to clarify other aspects of the problem. In our reply which follows, we discuss (A) the $E\mu\tau$ dependence of the steady-state photocurrent (Fig. 1), as pointed out by Dr. Spear, (B) the higher mobility electron current, (C) the concept of "impurity" band conduction, and (D) the

---

* The contents of this section is contained in a correspondence by me to Professor W. E. Spear, University of Leicester, Leicester, England.

experimental method used.

(A) With reference to your $\mu E\tau$ dependence, where τ is a lifetime, a clarification of the photogeneration process is necessary. For light whose energy $h\nu$ is near the band gap (3.82 ev, .325μ), all but a negligible number of photogenerated carriers are produced in a narrow region about .001 cm thick adjoining the illuminated surface. This penetration depth corresponds to 1% to 5% of the thickness of the specimens used here. This conclusion is based directly on the absorption coefficient, α in cm^{-1}, which is known to lie between 10^3 and 10^4 for radiation at the band gap. Thus for a sample .02 cm thick and $\alpha = 3.10^{+3}$ at the band gap frequency, the intensity of the light penetrating but 10% of the sample would be reduced to 1/400th of its initial value in this layer. Now, most assuredly, the rates of generating holes and electrons are equal, as they are generated across the band gap one electron for each hole, and their rates of recombination in this layer are equal as they recombine one for one. Consequently, the numbers of electrons and holes drawn into the bulk of the sample per unit time for the same applied field in the layer are the same, as you point out, independent of mobility. This rate is just equal to the difference of generation rate and recombination rate, and under steady-state conditions this net rate of flow out of the generation layer is just the observed current. This is true because in the bulk where there is only one carrier present, there can be no loss due to recombination, and in the steady state the rates of trapping losses are just equal to the rates thermal regeneration. Now to find the determinants of this current we observe that the ratio of the probability per unit time that an electron leaves the generation layer before recombining ($E\mu_e/\Delta x$) to the probability per unit time it recombines

$(1/\tau_{er})$ is $E\mu_e\tau_{er}/\Delta x$ where Δx is about half the thickness of the generation region and depends only on the wave length of the light. This is just your relationship with τ pinpointed. E is the electric field in the layer; τ_{er} is the recombination time of an electron, which depends proportionally on the number of holes in the layer, and τ_{hr} is that for a hole. Lifetimes for trapping are, of course, included in the mobilities and do not enter explicitly. The significant feature is that if the electrons were hopelessly trapped the resulting space charge would reduce E, the electric field in the layer, to such a low value that recombination would eliminate any observable photocurrent. (Note that with lower E, τ_{er} is also lowered owing to the presence of more holes and $E\mu_e\tau_{er}$ would then be small indeed.) Unfortunately, as you also pointed out, little else can be obtained from the relation $E\mu_e\tau_{er} \approx E\mu_h\tau_{hr}$, (where the fields in the layer are naively equated even for a constant applied voltage -- one expects different magnitudes of space charge in the bulk to alter this equality), because the τ_r's are strongly dependent on the steady-state hole and electron concentrations, which depend on the mobilities, etc. We have belabored this point to clarify our interpretation of the carrier generation, and again we thank you for calling it to our attention.

(B) But of greatest interest and concern between us is, of course, the high mobility electrons which we have studied. In the next few paragraphs we explain three reasons why the high mobility electron current we observe cannot be attributed to the backwards drift of holes generated at the opposite surface or in the bulk: (a) while <u>comparable</u> mobilities were observed for holes and fast electrons, these mobilities were never <u>equal</u>: they were in most cases significantly different beyond

the 5% experimental error -- had holes been in transit, the mobilities observed would have been equal; (b) the oscillographs of hole and fast electron charge transport versus time are different -- a small, initial transit of holes is observed in the case of fast electron transit; (c) the quantity of charge transported in the first few μ seconds is two or more orders of magnitude larger than that which would result from a back drift of holes from the surface opposite the illuminated one. We trust you will examine these arguments carefully: we feel our arguments for the fast electron current we observe are sound and strongly supported.

Owing to the orthorhombic crystal structure of α-sulfur (Fddd), in particular the inversion symmetry, the hole mobility in one direction must be equal to that in the opposite direction. (In fact, of course, time reversal symmetry implies that for any crystalline structure, mobilities in opposite directions must be the same.) So whether holes flow away from the illuminated surface, or are pulled toward it, the charge transport versus time oscillograms must yield the same mobility. But as is clearly evident from our results, especially samples M and X, the mobilities differ by factors of 1.5 and 3.0! While, to be sure, the mobilities for both holes and fast electrons varied widely from sample to sample, for any one sample, these two mobilities were easily and reproducibly measurable to 5% or better. For samples A through F, while no quantitative measurements were recorded, the hole current was always noted, and $1/\tau$ (τ = transit time) consistently differed (10% to 100% higher) from that of electron transport for the same field strength. We now by hindsight see the utility of making such measurements, but we felt and still feel your work with holes was sufficient.

For our second point, we emphasize graphically the significant differences between the charge transport versus time (Q vs. t) oscillographs for fast electrons and holes. For the same magnitude of the field, the fast electron transport nearly always rises less sharply in time than the hole transport, indicating the larger role which the traps play in electron transport. Furthermore, regarding the fast electron curves, the contribution of the holes to the transported charge is nearly always seen as an initial, steep slope on the Q vs. t oscillogram, representing 1% - 10% of the total charge transported. This was pointed out in Figure 4 and in article 3 of (14) and referred to in reference (4).

Referring now to Figure 7, here we have collected together the Q vs. t characteristics of a sample .022 cm thick (sample X) with an applied voltage of 200 volts from hole current and fast electron current oscillograms with time scales of .2, 1.0, 5.0, 20, 50, 200 μsec/cm, and slow electron current oscillograms at 500 μs/cm and 2000 μs/cm. For the positive field the hole transport (A) has a clearly defined transit time of 1.7 μsec. For the opposite polarity, the negative field, we have a 4% contribution at μ_h (B), followed by a well-defined electron transport which clearly exhibits <u>two</u> transit mechanisms (C and D). For times in the μsec range, the slope of the charge transport just subsequent to the hole contribution (E) is extrapolated to the charge asymptote (F) determined by the charge level in the 200μs-1000μs range to obtain a transit time for fast electrons of 6.1 μsec. Between 10μs and 400μs (not shown) the transported charge rises smoothly. In the msec range a second mobility is evident with a rise time of 6.8 - 0.6 = 6.2 msec. For each sample, such sequences of oscillograms were taken for voltages between 20V and 1300V, and each oscillograph

was repeated at least three times. Plots of $1/\tau$ versus V were made to obtain the mobilities: $\mu_h = 1.45$, $\mu_e = .40$, $\mu_{I.B.} = 4.0 \cdot 10^{-4}$, sample X in this case. Usually the "impurity" band (slow electron) current did not appear until voltages of about 10^3 or higher were applied, owing to the relatively low $\mu_{I.B.}$. Thus they were not determined as well as the one shown in Fig. 5 of (14), or the other two in Table I and were not listed. Our primary interest at the time was in μ_e, μ_L, E_t and N_t for the fast electrons. In as much as we see the contribution of holes in the charge transport for the negative fields so explicitly, and that the subsequent characteristic (.05 μsec to 10 μsec +) for this negative field clearly exhibits a more trap dominated flow of charge as well as a different mobility (factor of .3) than does the positive field transport, we cannot see how this can be explained as the reverse flow of holes from the other electrode.

As to our third point, notice that the fast electron mechanism has transported about one-sixth as much charge as the hole current for the opposite polarity. But even for a sample of .022 cm thickness, as used in this example, the contribution to the current due to holes excited at the opposite surface is completely negligible. For illumination near the band gap, (3.82 ev), the intensity of the light would have fallen by at least a factor of $e^{-20} \approx 4.10^{-8}$ ($10^3 \leq \alpha \leq 10^4$); for illumination around $\lambda = .39\mu$, where (based on Fig. 1 of (1) and (14) for D.C. photocurrents) the contributions to either current is down by 10^{-3}, the absorption of light in passing through the sample is still like e^{-4} to e^{-10}, $2.10^2 \leq \alpha \leq 5.10^2$. And even near $.43\mu$ where the absorption of light in the sample only reduces the intensity by a factor of e, the generated charge is still down by 2.10^{-4}. Yet the lowest the fast electron contribution was below the hole current for the opposite polarity was 1/50; a factor

of 1/6 to 1/10 was quite common. Thus on the basis of the comparable but distinctly different mobilities of holes and fast electrons, the explicit evidence of hole current in the initial phase of the electron current, its distinctly different contribution there, and the catastrophic attenuation of light near the band gap in the sample or similar reduction of carrier production below the band edge, we cannot help but conclude we are studying fast electron current in sulfur.

(A fourth observation, but only a qualitative one, also implies that we are observing fast electrons as opposed to reverse flowing holes. In the middle of the last paragraph of Article 2 of (14), we mention that we observe the presence of space charge left in deep traps by a transit of carriers. For both sign of carrier, the Q vs. t oscillographs for the fast current components decrease in amount of total charge transported between successive carrier transits to a steady-state level 5% to 20% below the initial level if the specimen is not neutralized in the interim (Fig. 8). [Neutralized sample means no carrier transport for zero applied field. All of our reported results were obtained from measurements made on samples neutralized after each transit of carriers. Thus, in addition, one cannot claim that holes were pulled into the sample owing to a negative space charge in the bulk.] But to continue, if now indeed holes flowing from the unilluminated surface were responsible for our fast electron current, the accumulation of electrons in deep traps in the bulk left by the successive transit of slow electrons would form a space charge that would increase the field for holes at the opposite surface, and thereby enhance the amount of transported charge for negative fields, instead of decreasing it, as is always the observed result. Note that reverse hole current would also

show a larger apparent mobility than μ_h because of the negative charge generated at the illuminated electrode. But the fast electron mobilities observed were in fact smaller than μ_h. [Note also that while the reverse hole transit (if it existed) would, of course, also deposit charge in traps; the magnitude is far outweighed by the amount left by the slow electrons.] The consistency of fast electron transport in the above four arguments is indeed strikingly good.)

(C) Designation of the electron trapping levels between .96 ev and 1.10 ev as an "impurity" band is undoubtedly a misnomer as you pointed out. And for such low mobilities as we both have found, hopping is indeed a plausible conduction mechanism: we thank you for communicating your results to us qualitatively. What we were referring to is that the energy of the electrons in this hopping is about 1 ev below the conduction band: we concluded that these slow electrons are in this "impurity" band as they transit the specimen. That the electrons are actually in this band rather than in the conduction band (fast electrons) was indicated by our avalanche phenomena. Briefly, the avalanche phenomena for electron transport are interpreted as being due to electronic excitation from the "impurity" band to the conduction band triggered by electrons in the conduction initially. This is based essentially on the observation that light at 1 ev (1.24μ) eliminates the avalanching (see Article 4 of (14)). Thus, as the avalanche requires a large concentration of electrons to be developed in the "impurity" band (partially to create the needed field strength), and that this concentration could easily be eliminated by photo-excitation at 1 ev, a likely mechanism for transport, in view of the fast electron current already present in the conduction band, would be conduction in this "impurity" band, possibly

by the hopping you suggest.

(The term "impurity" band is derived from the impurity levels in the forbidden band of semiconductors, which arise from donor and acceptor impurities. Hence, a level in the band gap of any crystalline material is referred to as an "impurity" level, and, if of sufficient density, it spreads into an "impurity" band. This terminology is common in discussing band structure in the electronic sense as we do in (1) and (14). In fact, one commonly says that holes (usually) move in the valence band, whereas in reality "they" move in their own conduction band! In sulfur these could be due to impurities, to defects, or be as you assert an intrinsic property of the material itself. We do not know, but your extensive and beautifully consistent results dealing with the slow electrons are very suggestive of your conclusion. But actually, to refer to trapping (or any other electronic process for that matter) in molecular crystals in terms of band structure is unfortunately misleading, because, as you point out, conductivity arises from molecular excited states as opposed to crystal excited states. However, inasmuch as the characterization of electronic properties in terms of a band structure is still possible, its use is most convenient.)

Regarding your experiments, especially with respect to the slow electron mobility you have studied in such detail,[15] the remarkable consistency in the temperature dependence of this mobility which you point out indeed seems fundamental: it was truly worthwhile that you pursued your investigations to this extent. You have found a thermal activation energy of .17 ev for this low mobility electron current, and your interpretation in terms of a phonon-assisted hopping mechanism is indeed plausible, as mentioned before. What we propose, however,

again on the basis of (a) the presence of fast electron transport in the conduction band, (b) the features of the avalanche phenomena previously described and (c) the prominence of levels displayed in the D. C. photocurrent versus wavelength curve for holes (Fig. 1 of (1) and (14)), is that this slow conduction is confined to the narrow region of levels between .96 ev and 1.10 ev (you would say around .94 ev, but this is immaterial). Mott and Twose[9] discuss such conduction: the theory is based on the overlap between localized electron wave functions in neighboring donor sites, and shows how the increase in the density of such sites lowers the activation energy from the common $(E_c - E_d)$ for very low density to a much lower value, approaching metallic conductivity in the limit. Again, we are <u>not</u> saying these levels originate from <u>impurities</u>: we do not know the origin of these levels. They exist, and your important findings add significantly to the hypothesis that these levels, with a .17 ev activation energy, give rise to the slow mobility current.

(D) With respect to your search for the high electron current, we fully realize the difficulties encountered in obtaining an electron beam of sufficiently high density and yet of sufficiently low energy to generate appreciable numbers of electrons for transit without these being totally masked by holes produced in the bulk. And since you are doing such an extensive amount of work with sulfur, and most likely with other similar materials in the years to come, may we suggest you try using a "Fischer-Nanolite", or similar ultra-fast, high-intensity light source, in addition to your electron beam and other flash methods, to photogenerate the carriers. To use this light source is simplicity itself; the reproducibility is fantastic; the half-width of 10 nsec in the

intensity, 10%-width of 36 nsec, enables one, for example, to look back to 50 nsec to clearly distinguish the initial hole current when studying electron transport. If you are interested, the main references are the following: Heinz Fischer, Journal of the Optical Society of America, 51, 543, (1961); Chemie-Ingenieur Technik 34, 118, (1962); and p. 152 ff of the Sixth International Congress on High-Speed Photography, The Hague-Scheneninger, Sept. 1962. The address for further information is Impulsphysik, Dr. -Ing. Frank Früngel GmbH, Hamburg-Rissen, Sülldorfer-Landstr. 400, Germany. We have found the instrument invaluable in studying semi-conducting materials as well.

After communicating the above to Dr. Spear, November 8, 1965, on December 16, 1965, we received word from Dr. William Gill (IBM Research Laboratory, San Jose, California) that, by using yet another method, he too had observed the higher mobility electrons in three samples. His method of observing transient space-charge-limited current (8) excited by a burst of laser light also fixed the sign of the charge carriers unambiguously. He also reported that the mobilities of the holes and fast electrons fluctuated from sample to sample (1.0- 10. cm^2/V-sec), but the low electron mobility was reasonably stable around 4. - 5. $\cdot 10^{-4}$ cm^2/V-sec. However, no further results have been published.

I.6. Conclusions

By analyzing the transport of electrons and holes in α-sulfur using transient drift mobility and d. c. photoconductive techniques, a consistent picture of the energy gap of sulfur has been developed. Comparable values of room temperature electron and hole mobilities of the order of 1-4 cm^2/V-sec were found, along with a low electron

mobility current at 4×10^{-4} cm^2/V-sec. Three different methods were employed to measure the effective shallow trapping level of the electrons (0.12 ± 0.01 eV), and a trapping density of about 3×10^{17} cm^{-3} was found. The deep trapping level for electrons was also confirmed by a third measurement (1.0 eV below the conduction band). An avalanching phenomenon was also treated and found consistent with the model proposed for energy gap of sulfur.

I.7. Note Regarding Theory

Charge carriers are created near one of the surfaces of a flat thin piece of insulating material and depending on the applied bias, holes or electrons can be drawn across the sample. The transit is observed by measuring the total induced charge on one of the electrodes as a function of time.

Assumptions suggested by experimental results are the following:

I. Planar geometry.

II. No injected carriers: the neutralized samples could be held in the dark for hours at ± 1000 V with no perceivable change in space charge.

III. A very large dielectric relaxation time:

$$\tau_d = \epsilon/\sigma \quad , \quad \epsilon = 4\epsilon_0 \quad , \quad \sigma = 5 \cdot 10^{-16}\ \Omega\text{-m} \quad , \quad (12)$$

$$\therefore \tau_d = 7 \cdot 10^4 \text{ sec.}$$

IV. The hole and electron mobilities are independent of the electric field: there was no appreciable deviation from linearity of $1/\tau$ versus V for large V, where τ is the transit time and V is the applied voltage.

V. Large carrier lifetimes: after the photo-generated carriers have separated, there is little chance for recombination, as we have

only a one carrier problem. Trapping and thermo-regeneration times may be any value, however.

VI. In addition to relatively shallow traps which alter the "lattice" mobility μ_L, deeper traps exist which trap carriers with probability $1/\tau_t$ and release them with probably $1/\tau_r$. Hence below "free" means that the carrier is either in the conduction (or valence) band or in a "shallow" trap from which it is thermally excited at a much higher rate than it would be for deeper trapping.

Consider two flat parallel electrodes of infinite extent at x = 0 and x = d. Then the charge q' induced on the electrode at x = 0 due to a charge q at x is given by

$$q' = -q\,\frac{d-x}{d} \tag{A-1}$$

Hence the current into that electrode is given by

$$i = \frac{dq'}{dt} = q\,\frac{V_x}{d} = q\,\frac{\mu V}{d^2} = q/\tau \tag{A-2}$$

where μ is the shallow-trap controlled mobility and τ is the transit time if no deep traps are present. We now have the essential result that the contribution of each charge to the current into one electrode depends only on whether it is free or bound: if free it contributes q/τ, if bond 0, independent of its position. Thus the charge Q_T measured at time t on the electrode at x = 0 is just

$$Q_T(t) = \frac{1}{\tau}\int_0^t Q_f(t)\,dt \;; \quad Q_f(t) = Q_0 - Q_t(t) \tag{A-3}$$

where $Q_f(t)$ is the total free charge in the sample, $Q_t(t)$ the total charge in deep traps, and Q_0 the initial photogenerated charge.

The relations between $Q_f(t)$ and $Q_t(t)$ are approximately:

$$\frac{dQ_f}{dt} = -\frac{Q_f}{\tau_t} + \frac{Q_t}{\tau_r} - \frac{Q_f(t-\tau)}{\tau}\,u(t-\tau) \qquad \text{(A-4a)}$$

$$\frac{dQ_t}{dt} = -\frac{Q_t}{\tau_r} + \frac{Q_f}{\tau_t} \qquad \text{(A-4)}$$

where

$$u(x) = 0 \quad x<1$$
$$= 1 \quad x>1$$

The third term on the right represents the flow of charge out of the sample. It states that the efflux of charge at t is proportional to the free charge in the sample at $t - \tau$. As may be checked by the final value theorem for Laplace Transformations, the time constant for this process τ, ensures that $Q_T(t) \to Q_0$ as $t \to \infty$.

The solution of these Equations via Laplace Transforms for $t < \tau$ is straightforward and gives, since $Q_f(0) = Q_0$, $Q_t(0) = 0$

$$Q_f(t) = Q_0\,(A + B e^{-t/\tau_0}) \qquad \text{(A-5)}$$

where $A = \tau_0/\tau_r$, $B = \tau_0/\tau_t$, $1/\tau_0 = 1/\tau_r + 1/\tau_t$ and hence,

$$Q_T(t) = \frac{Q_0}{\tau}\left(At + B\tau_0(1 - e^{-t/\tau_0})\right) \quad \text{for } t \le \tau \qquad \text{(A-6)}$$

If we let the thermo-release time τ_r become very large, we have just the Hecht formula.[13] Notice that from (A-3) we have

$$\frac{dQ_T}{dt} = \frac{Q_f}{\tau} \qquad \text{(A-7)}$$

hence the equation for the initial slope is just

$$Q_T' = \frac{Q_o}{\tau} t$$

and the intersection of the tangents now occurs at

$$t' = A\tau + B\tau_o(1-e^{-\tau/\tau_o}) \qquad \text{(A-8)}$$

Several limiting cases are of interest:

Case 1: $\tau \ll \tau_t \ll \tau_r$ This case corresponds to hole transport where using Adams and Spear[2] $\tau_t \approx 10^{-5}$ sec, and for the mobilities found there $\tau \approx 2.10^{-7}$ sec at 1000 V. τ_r was of the order of minutes.

$$Q_T \approx \frac{Q_o}{\tau} t \;,\; t \le \tau \;;\; \text{and} \quad Q_T \approx Q_o \;,\; t > \tau .$$

As would be expected and as was usually observed, the charge induced rises almost linearly at the initial rate to the maximum value. Curves of this are shown in Ref. (7).

Case 2: $\tau_t \ll \tau \ll \tau_r$ This case corresponds to electron transport where again using Adams and Spear[2] $\tau_t \approx 5.10^{-9}$ sec, $\tau_r \approx 32$ min, and again $\tau \approx 2.10^{-7}$ sec. Now $Q_T \approx Q_0(\tau_t/\tau)\,(1-e^{-t/\tau_t})$ for $t \ll \tau$, so that the linear part has a much shorter duration, and appreciably fewer charge carriers would be observed. Using a solution for $t > \tau$, the charge time characteristic can still be used to determine τ. Alternatively τ might be made comparable to τ_t by increasing the applied field.

Case 3 and 4: $\tau_r \ll \tau_t \ll \tau$, $\tau_r \ll \tau \ll \tau_t$; These cases may be viewed as shallow trapping effects. Then

$$Q_T \approx \frac{Q_o}{\tau} t\,(1+\tau_r/\tau_t) \approx \frac{Q_o}{\tau} t \quad \text{for} \quad t \le \tau$$

$$\approx Q_o \quad \text{for} \quad t > \tau$$

which is the same result as Case 1. Thus we obtain the result that if the release time is much less than the transit and trapping times, the charge-time characteristic for transit times less than or greater than trapping times are nearly identical. This, moreover, corresponds to the result for a long release time and $\tau << \tau_t$, as is intuitively evident.

Table I

Sample	μ_h	μ_e	E_t	N_t	μ_L	$\mu_{I.B.}$
M	5.0	3.6	-	-	-	-
G	5.0	4.8	-	-	-	-
X	1.45	0.40	-	-	-	4×10^{-4}
Y	0.65	0.005	-	-	-	9×10^{-5}
A	-	1.1	-	-	-	-
B	-	1.2	-	-	-	-
C	-	0.70	0.11 eV	3.5×10^{17}	1.5	-
D	-	1.92	0.12 eV	2.8×10^{17}	4.0	-
E	-	1.3	-	-	1.3	1.2×10^{-3}
F	-	0.87	0.13 eV	3.0×10^{17}	2.4	-

Table 1. Table of values found for the room temperature hole mobility μ_h ($cm^2/V\text{-}sec$), room temperature electron mobility μ_e ($cm^2/V\text{-}sec$), E_t effective level of electron traps controlling the mobility, N_t the density of these traps (cm^{-3}), μ_L room temperature electron lattice mobility ($cm^2/V\text{-}sec$), $\mu_{I.B.}$ room temperature electron impurity band mobility ($cm^2/V\text{-}sec$).

Figure Captions

Fig. 1. Photo-response of an Au-α sulfur - Au sample, thickness .02 cm, biased to 300 V. Δ-hole current, 0-electron current.

Fig. 2. Upper curve, electron transport, 700. V negative bias; lower curve, hole transport, zero bias, field due to trapped electrons. Horizontal scale 10μ sec/cm, vertical scale $0.3 \cdot 10^{-12}$ Coul/cm. In several samples the electron charge rose as sharply as that for holes.

Fig. 3. Typical I-V characteristics for D. C. illumination at $\lambda = .275\mu$. Electron current has been increased by a factor of ten to ease comparison.

Fig. 4. An example of low mobility electron transport versus time at 10 KV/cm. The first 1/2 msec of the trace represents high mobility electron current. Upon going to sweep speeds of 5μs/cm a 4% initial, rapid transit of holes was recorded. Horizontal scale 2msec/cm, vertical scale $0.4 \cdot 10^{-12}$ Coul/cm.

Fig. 5. Graph of reciprocal transit time, $1/\tau$, versus negative applied potential for low mobility electron current.

Fig. 6. A portion of an electron avalanche characteristic. Applied field is -1300 volts across a .025 cm sample. Horizontal scale .1 m sec/cm, vertical scale 5 nAmp/cm.

Fig. 7. Transported charge versus time for holes, fast electrons and slow electrons. Sample X, .022 cm thick, $\mu_r = 1.45$, $\mu_e = .40$, $\mu_{I.B.} = 4.0 \cdot 10^{-4}$.

Fig. 8. In which the effect of the accumulation of charge in the sample on the charge transport is shown.

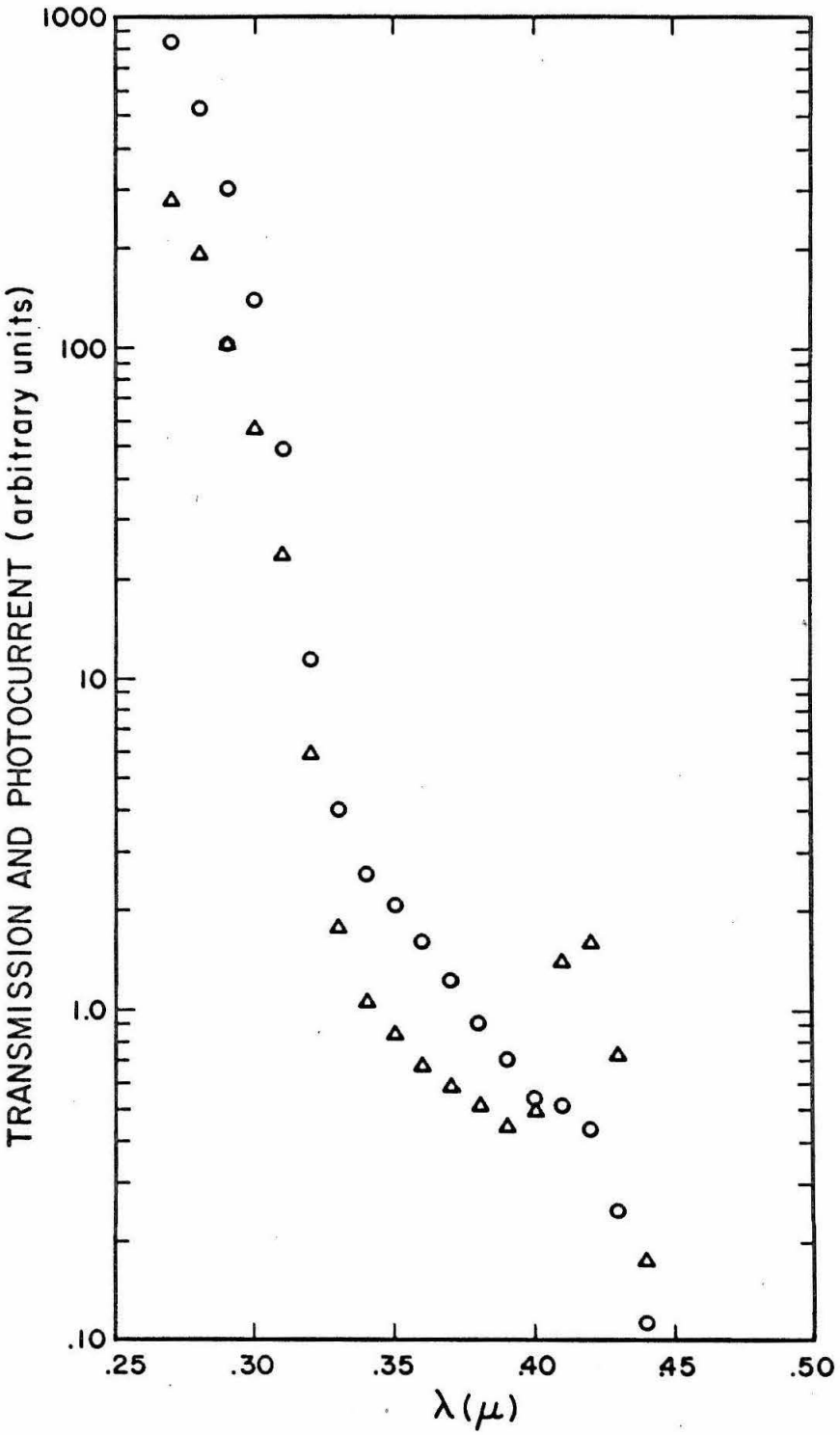
1000
100
10
1.0
.10
TRANSMISSION AND PHOTOCURRENT (arbitrary units)
.25
.30
.35
.40
.45
.50
λ(μ)

FIGURE 1

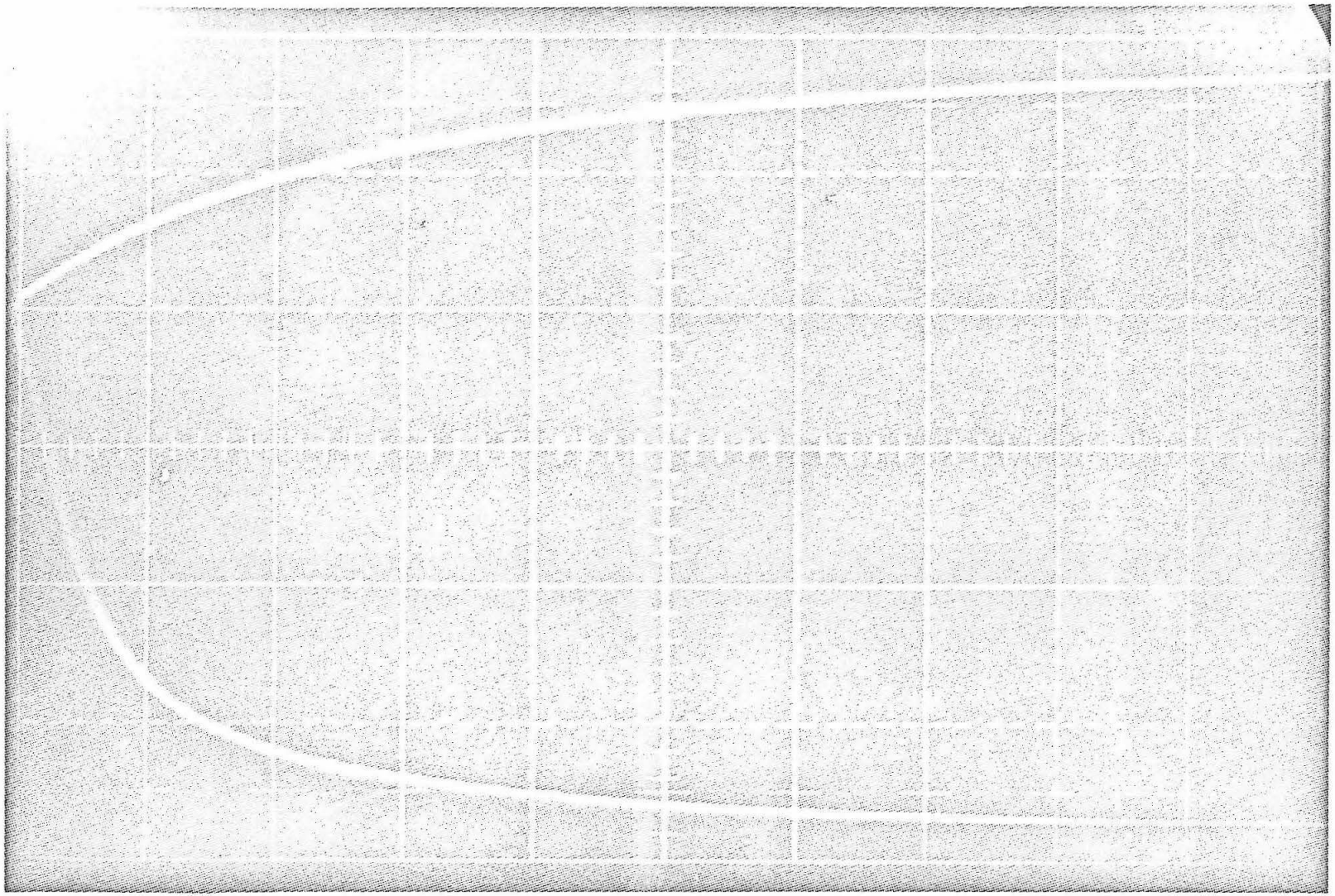

FIGURE 2

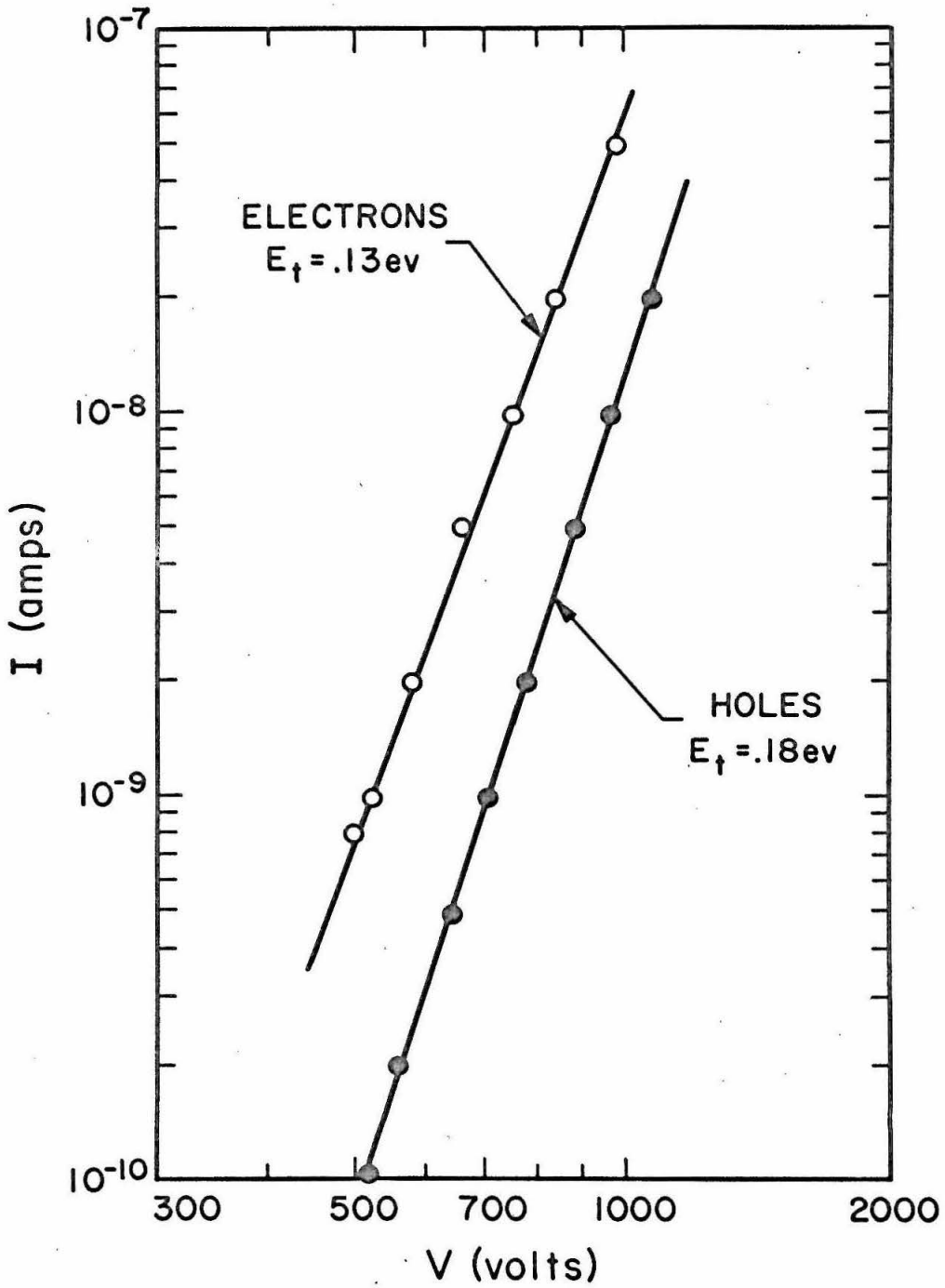
10^{-7}
10^{-8}
10^{-9}
10^{-10}
I (amps)
ELECTRONS
E_t = .13ev
HOLES
E_t = .18ev
300
500
700
1000
2000
V (volts)

FIGURE 3

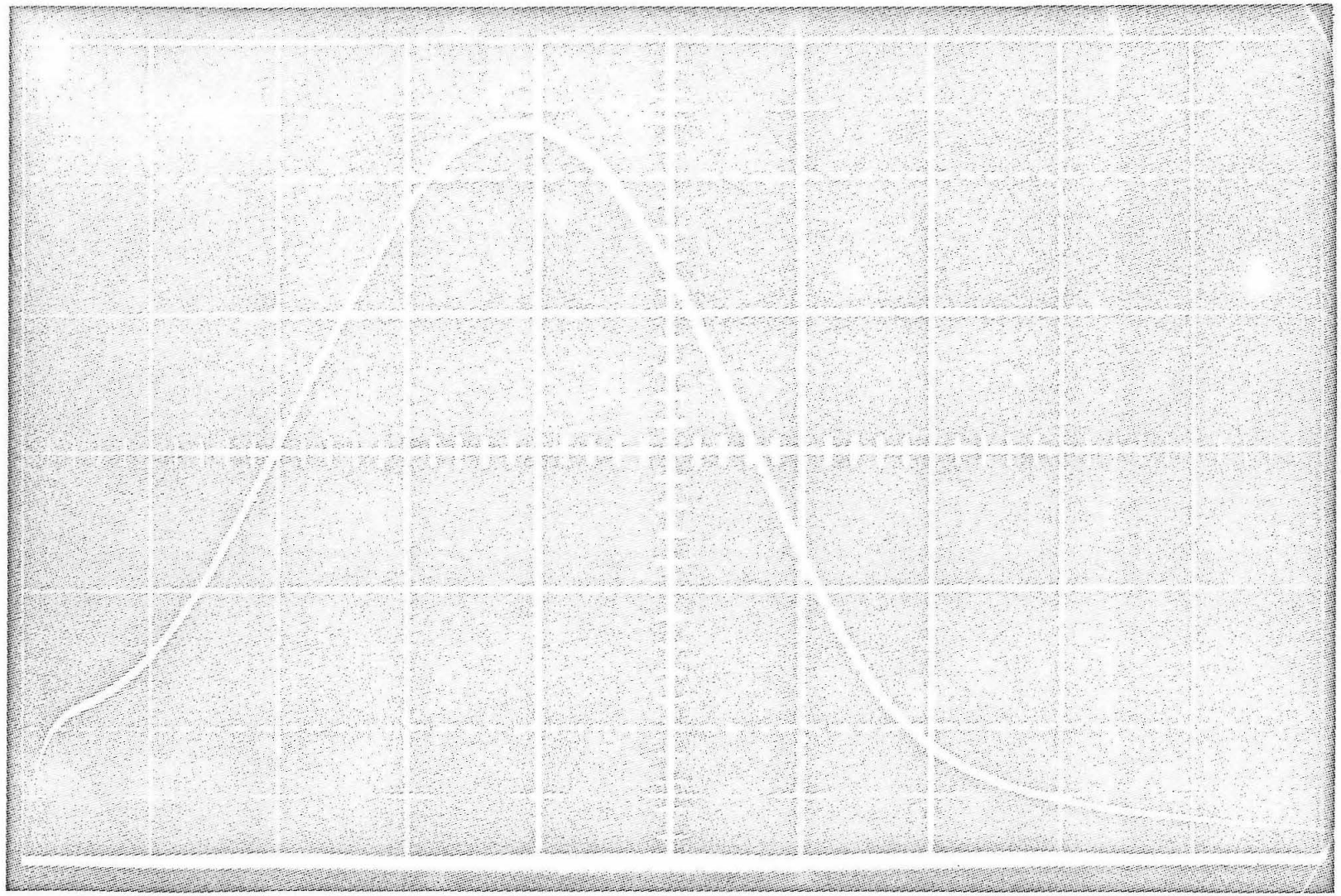

FIGURE 4

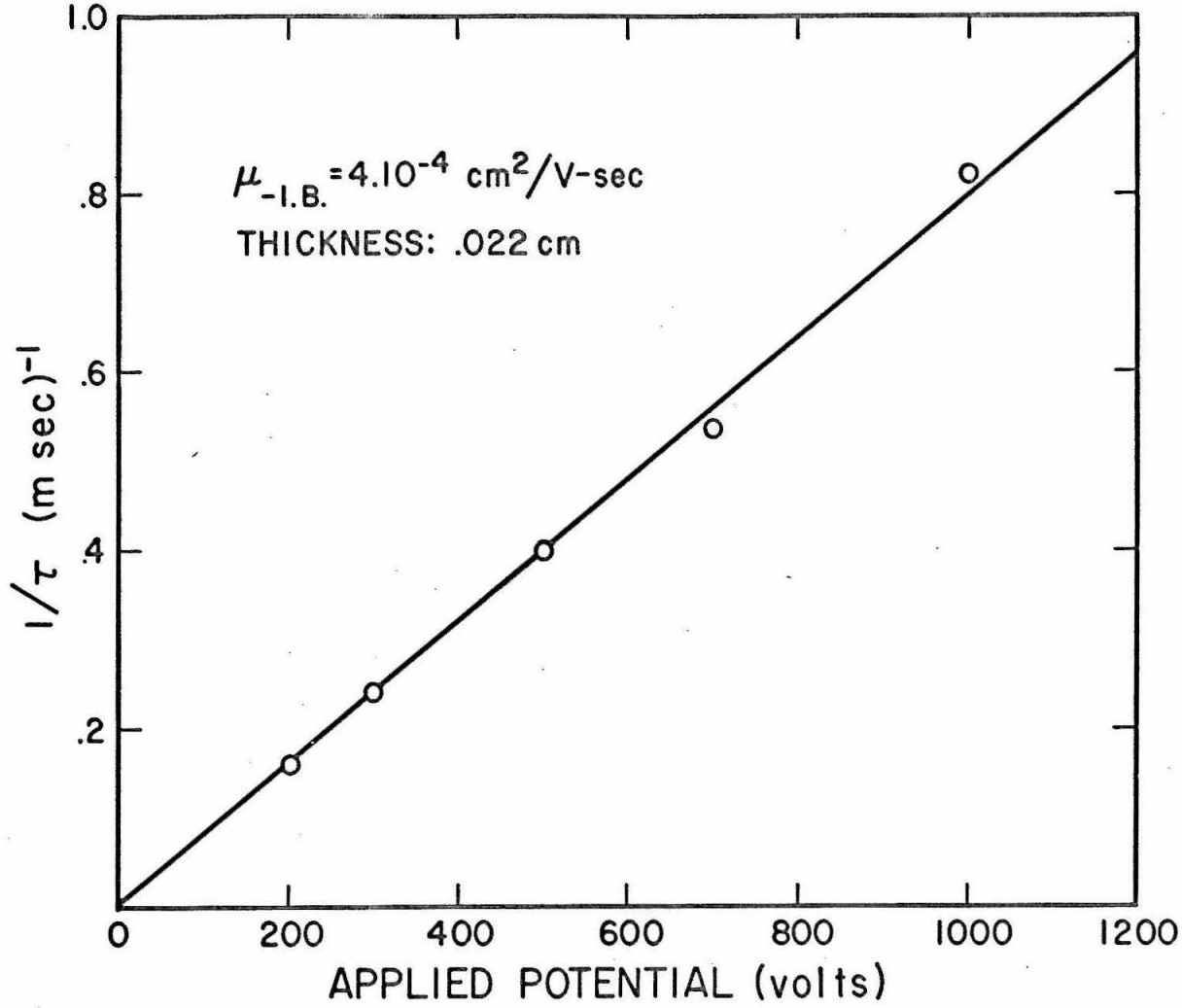
1.0
.8
.6
.4
.2
$\mu_{-I.B.} = 4.10^{-4}$ cm^2/V-sec
THICKNESS: .022 cm
$1/\tau$ (m sec)$^{-1}$
0
200
400
600
800
1000
1200
APPLIED POTENTIAL (volts)

FIGURE 5

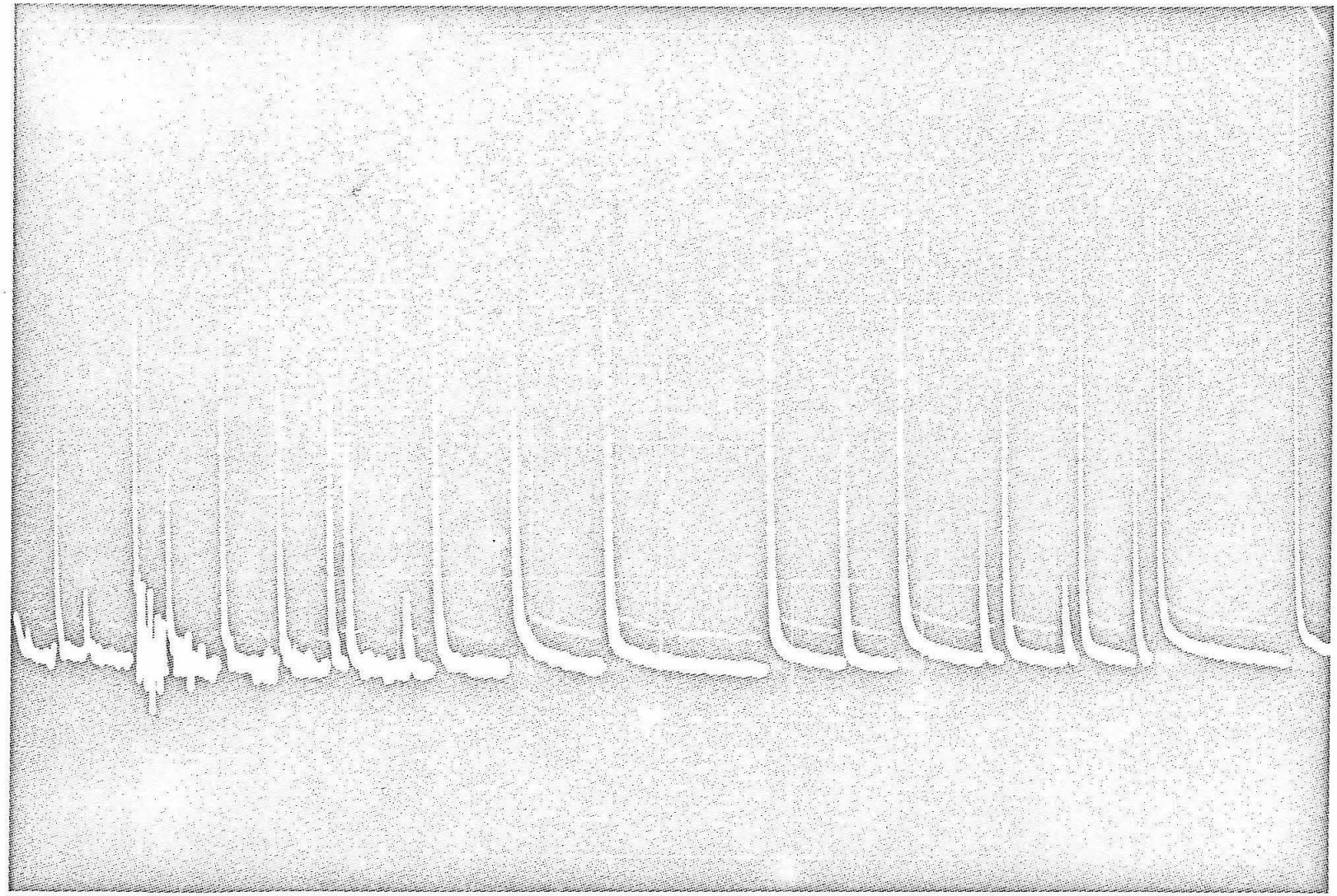

FIGURE 6

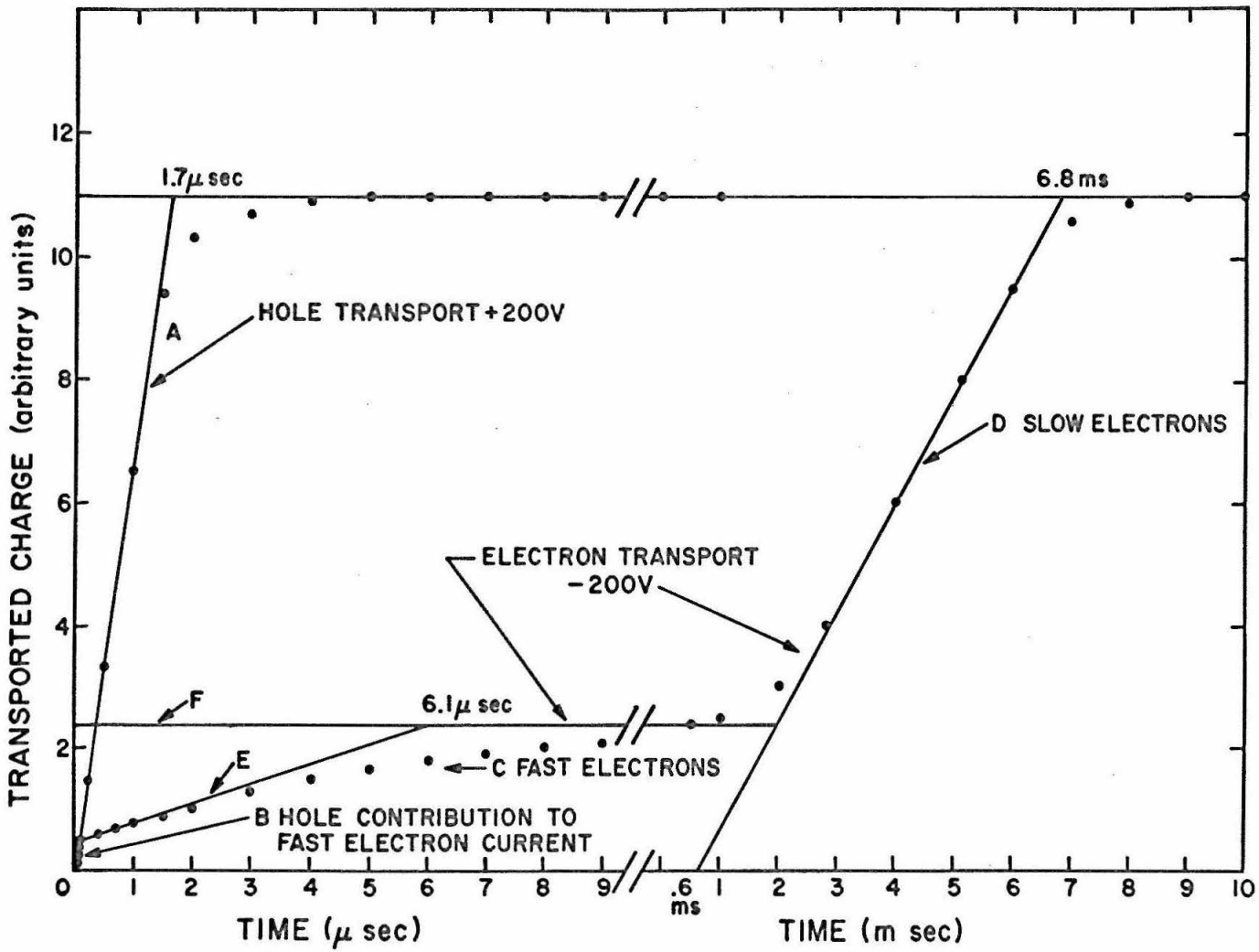
TRANSPORTED CHARGE (arbitrary units)
12
10
8
6
4
2
0
1.7μ sec
6.8 ms
HOLE TRANSPORT +200V
A
D SLOW ELECTRONS
ELECTRON TRANSPORT
-200V
F
6.1μ sec
E
C FAST ELECTRONS
B HOLE CONTRIBUTION TO
FAST ELECTRON CURRENT
1 2 3 4 5 6 7 8 9
.6 ms
1 2 3 4 5 6 7 8 9 10
TIME (μ sec)
TIME (m sec)

FIGURE 7

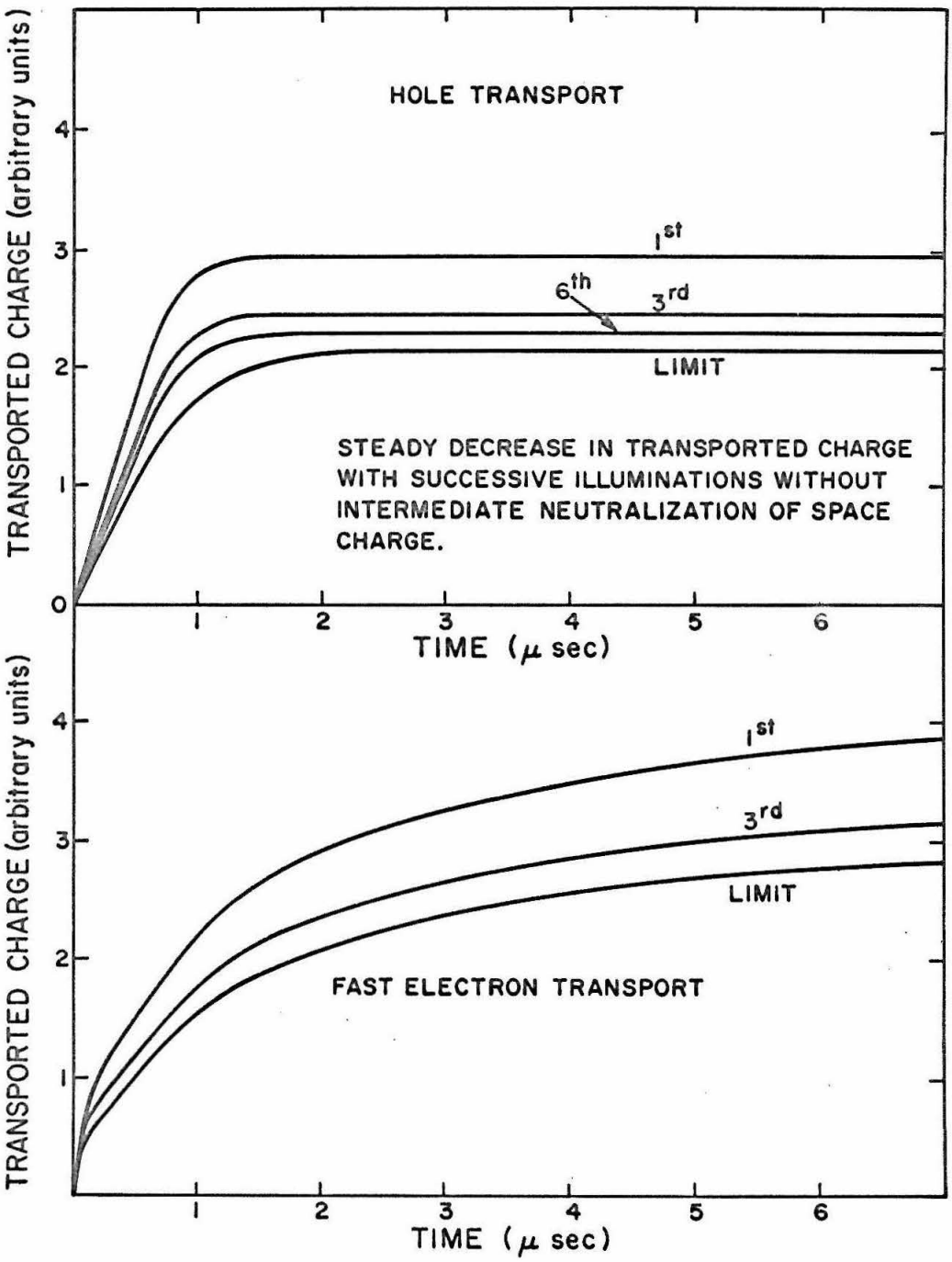
HOLE TRANSPORT
TRANSPORTED CHARGE (arbitrary units)
1st
6th
3rd
LIMIT
STEADY DECREASE IN TRANSPORTED CHARGE WITH SUCCESSIVE ILLUMINATIONS WITHOUT INTERMEDIATE NEUTRALIZATION OF SPACE CHARGE.
TIME (μ sec)
FAST ELECTRON TRANSPORT
TRANSPORTED CHARGE (arbitrary units)
1st
3rd
LIMIT
TIME (μ sec)

FIGURE 8

References for Part I

1. Mead, C. A., Phys. Letters 3, 212 (1964).

2. Adams, A. R. and Spear, W. E., J. Phys. Chem. Solids 25, 1113 (1964).

3. Dean, P. J. et al., Proc. Phys. Soc. 75, 119 (1960).

4. Spear, W. E., Proc. Soc. London B20, 669 (1957).

5. Spear, W. E., Proc. Phys. Soc. London 76, 826 (1960).

6. Spear, W. E., J. Phys. Chem. Solids 21, 110 (1961).

7. Spear, W. E. and Mort, J., Proc. Phys. Soc. 81, 130 (1963).

8. Rose, A., Concepts in Photoconductivity and Allied Problems, Chapt. 4, Interscience, New York (1963).

9. Mott, N. F. and Twose, W. D., Advances in Physics, Vol. 10, p. 107, Taylor and Francis, London (1961).

10. This result was determined independently by Adams and Spear[2] who found the level to be 0.94 eV below the conduction band by an elegant experiment in which the thermal release time of the deeply trapped electrons was measured versus temperature. The possibility of impurity band conduction in CdS has been considered previously.[7]

11. Haitz, R. H., J. Appl. Phys. 35, 1370 (1964).

12. Moss, T. S., Photo-conductivity in the Elements, p. 180 ff. Butterworths, London (1952).

13. Hecht, K., Z. Phys. 77, 235 (1932).

14. Thornber, K. K. and Mead, C. A., J. Phys. Chem. Solids, 26, 1489 (1965).

15. Adams, A. R., Gibbons, D. J., and Spear, W. E., Solid State Comm. 2, 387 (1964).

PART II

POLARON MOTION IN A D.C. ELECTRIC FIELD

I. Introduction

In this paper we treat the motion of an electron in a polarizable crystal at arbitrary temperature subjected to an arbitrary, D.C. electric field. The coupling of the electron to the lattice is also arbitrary. Many authors have already treated other aspects of the polaron problem.[1-5] Here we find a rather simple explicit relationship between the electric field strength in the lattice and the expectation value of the velocity of the electron.

In carrying out the solution, we maintain the standard polaron model of the electron coupled only to the optical phonons. The crystal with electric field is assumed to be initially in thermal equilibrium, and the steady-state, translational motion of the electron subsequent to its injection into the lattice is determined. Phonons emitted from (or absorbed in) the polaron are assumed to propagate away to infinity without interacting with the phonons already present in thermal equilibrium. If the electric field is so strong as to alter the frequency of the optical modes, it is these new frequencies that we must use in our expressions.

Using this model we present two approaches for the solution of the problem. In the first we find the expectation value of the displacement of the electron using Feynman's Path Integral method. The coordinates of the lattice oscillators are easily eliminated. But since we cannot perform the path integrals over

electron coordinates exactly, we approximate the effective lattice potential by an arbitrary distribution of oscillators, and then carry out a perturbation approach similar to that of Reference 2 (FHIP). But we emphasize that this perturbation approach does not involve an expansion in the electric field: the electric field term is never approximated. Having obtained the expectation value of the displacement, that of velocity follows immediately from differentiation.

The second approach involves equating the expectation value of the rate of loss of electron momentum to the lattice to the electric field. The use of time rates of change from the outset is a more direct and useful procedure in steady state, non-equilibrium processes.

Finally, we present plots of electric field versus electron velocity calculated for a simple distribution of oscillators for coupling constants of $\alpha = 3$ and $\alpha = 7$. The results are not only physically realistic, but point toward difficulties to be encountered if one desires to accelerate electrons to energies above the rest-strahl energy in polarizable crystals.

II. First Approach -- Electric Field-Velocity Relationship from the Expectation Value of the Displacement of the Electron.

A. Outline of the Method

To determine the displacement in time of an electron in a polarizable crystal in a uniform, static, electric field, we proceed as follows. First the expectation value of the displacement of the electron is cast into the form of a Feynman Path Integral, from which all the coordinates associated with the lattice can be eliminated exactly, leaving only the coordinates of the electron. Then the action in the path integral is approximated by a distribution of harmonic oscillators, which enables us to expand the displacement in a power series in terms of the difference between the exact and approximate actions. Using an expansion motivated by an exact summation of such a series for a similar problem, we rewrite our series expansion in a form which more accurately represents the physics of the problem. Finally, a comparison of this result with various special cases which can be solved by other means leads directly to the final expression.

B. The Expectation Value of the Displacement of the Electron

If we let ρ be the density matrix of our electron-lattice system and x the position operator, then the expectation value of the displacement of the electron at time t, $\langle x(t) \rangle$, given that its value at t=0 is zero, is

$$\langle x(t) \rangle = Tr\,(x(t)\rho) = Tr\,(x\,\rho(t)) \qquad (1)$$

For thermal equilibrium problems, one can use $\rho=\exp(-\beta H)$, where $\beta=1/kT$ and H is the Hamiltonian of the system. In our problem, however, only $\rho(0)=\exp(-\beta H)$, because we have assumed thermal equilibrium initially. To determine the density matrix for $t>0$, we solve its time-evolution equation

$$i\hbar \frac{\partial \rho}{\partial t} = [H, \rho] \tag{2}$$

and therefore

$$\rho(t) = e^{-i/\hbar \int_0^t H(s)\, ds} \rho(0) e^{i/\hbar \int_0^t H'(s')\, ds'} \tag{3}$$

Here the time-ordered operator notation is used: unprimed operators to the left and ordered right to left with increasing time, and primed operators to the right and ordered left to right with increasing time.

The Hamiltonian appropriate for an electron interacting with the longitudinal optical modes of an at least partially ionically bound crystal in an electric field, which preserves the essential physics of the problem, is

$$H = \bar{p}^2/2m - \bar{F}(t)\cdot\bar{x} + \sum_{\bar{k}} \omega_{\bar{k}} a_{\bar{k}}^{\dagger} a_{\bar{k}} + V^{-\frac{1}{2}} \sum_{\bar{k}} \left(C_{\bar{k}} a_{\bar{k}} e^{i\bar{k}\cdot\bar{x}} + C_{\bar{k}}^{*} a_{\bar{k}}^{\dagger} e^{-i\bar{k}\bar{x}} \right) \tag{4}$$

where $a_{\bar{k}}^{\dagger}$, $a_{\bar{k}}$ are the creation and annihilation operators of phonons of momentum $\bar{k}$, frequency $\omega_{\bar{k}}$, coupled to the electron via $\bar{p}$ is the momentum of the electron, m is its effective mass in a fixed lattice, $\bar{x}$ is its position coordinate, V is the crystal volume, e the magnitude of the electric charge on the electron, $\bar{F}(t)=-e\bar{E}(t)$,

and $\bar{E}(t)$ is the electric field in the crystal. In Fröhlich's model,[3]

$$C_{\bar{k}} = \frac{-i\hbar w_{\bar{k}}}{k} \cdot \left(\frac{\hbar}{2m w_{\bar{k}}}\right)^{1/4} \cdot (4\pi\alpha)^{1/2} , \qquad (5)$$

where

$$\alpha = \frac{e^2}{\hbar}\left(1/\epsilon_\infty - 1/\epsilon_0\right) \cdot \sqrt{\frac{m}{2\hbar w_{\bar{k}}}} . \qquad (6)$$

We maintain the usual convention of setting $\hbar = 1$, working with a unit volume, and incorporating the e into the $\bar{E}(t)$ so that $-e\bar{E}(t) \rightarrow \bar{E}(t)$. $\omega_{\bar{k}}$ is 2π times the frequency of the <u>longitudinal</u> optical phonon branch.

To evaluate (1) we note that since the energy of the electron and its interaction with the lattice is completely negligible compared with that of the heat bath, we may set

$$\rho(0) = exp\left(-\beta \sum_{\bar{k}} w_{\bar{k}}\, a^+_{\bar{k}}\, a_{\bar{k}}\right) \qquad (7)$$

as in FHIP.[4] (If one questions the validity of this approximation, or in fact the entire approach, for zero temperature (infinite β), he may compute the expectation value directly without resorting to statistical means, because in this case the initial wave function for the lattice as well as for the electron is known. The result of such a computation gives the $\beta = \infty$ limit of our solution here.)

The problem of integrating $Tr(\rho(t))$ over the crystal oscillator coordinates has been solved in references (2) and (5). If we replace $\bar{F}(t)$ in equation (3) by $\bar{F}(t) = \bar{E}(t) + \hat{x}L\delta(t - t_2^-)$, then

$$\langle X(t_2)\rangle = \frac{1}{i}\left|_{L=0}\right. \frac{\partial}{\partial L}\, Tr\left(\rho(t_2)\right) \qquad (8)$$

(Note that we still hold $\bar{F}'(t) = \bar{E}(t)$: $Tr(\rho(t))$ has conveniently been performed for different $\bar{F}(t)$, $\bar{F}'(t)$.) When converted to a path integral, $Tr(\rho(t_2))$ assumes the form

$$Tr(\rho(t_2)) = \iint e^{i\mathcal{L}_e}\, \mathcal{D}(\bar{X}(t))\, \mathcal{D}(\bar{X}'(t)) \qquad (9)$$

where

$$\mathcal{L}_e = \int_0^{t_2}\left(\tfrac{1}{2} m\dot{\bar{X}}^2(t) + \bar{F}(t)\cdot\bar{X}(t)\right)dt - \int_0^{t_2}\left(\tfrac{1}{2} m\dot{\bar{X}}'^2(t) + \bar{F}'(t)\cdot\bar{X}'(t)\right)dt$$

$$+ i\int \frac{d^3K}{(2\pi)^3}\,|C_{\bar{k}}|^2 \int_0^{t_2} dt \int_0^{t} dt' \Big[R_{\omega_{\bar{k}}}(t-t')\, e^{i\bar{K}\cdot(\bar{X}'(t)-\bar{X}'(t'))} + R^*_{\omega_{\bar{k}}}(t-t')\, e^{i\bar{K}\cdot(\bar{X}(t)-\bar{X}(t'))}$$

$$- R_{\omega_{\bar{k}}}(t-t')\, e^{i\bar{K}\cdot(\bar{X}(t)-\bar{X}'(t'))} - R^*_{\omega_{\bar{k}}}(t-t')\, e^{i\bar{K}\cdot(\bar{X}(t')-\bar{X}'(t))}\Big] \qquad (10)$$

and

$$R_{\omega_{\bar{k}}}(t-t') = \frac{e^{i\omega_{\bar{k}}(t-t')}}{1-e^{-\omega_{\bar{k}}\beta}} + \frac{e^{-i\omega_{\bar{k}}(t-t')}}{e^{\omega_{\bar{k}}\beta}-1} \qquad (11)$$

Although equation (10) represents quite a simplification in that the oscillator coordinates have been eliminated from (1) and (4) exactly, we know of no way to perform the last two path integrals. Thus we must use an approximate method, taking care to ensure that the electric field term in the action (or Hamiltonian) is not altered.

C. The Method of Approximation

The method of approximation that is physically a very reasonable one and that has worked particularly well on two prior occasions[1, 2] is to replace $\int \frac{d^3k}{(2\pi)^3}\,|C_{\bar{k}}|^2\, e^{i\bar{K}\cdot\bar{r}}$,

which is a 1/r potential for the Frȍhlich Hamiltonian, by a harmonic oscillator potential r^2. This means replacing, for example, the term $R_{w_k}(t-t') \int \frac{d^3k}{(2\pi)^3} |C_k|^2 e^{-i\bar{k}\cdot(\bar{x}'(t)-\bar{x}'(t'))}$ in the exact action Φ_e, which is $\frac{\alpha}{\sqrt{2}} R_{w_k}(t-t') \cdot |\bar{x}'(t)-\bar{x}'(t')|^{-1}$ for the Frȍhlich case, by $\frac{\alpha A}{\sqrt{2}} R_{\Omega}(t-t') (\bar{x}'(t)-\bar{x}'(t'))^2$. The relative strength of the oscillator, -A, and its frequency Ω, can in some cases be rigorously chosen by the criterion that the free energy of the system is a minimum. For our problem it proved expedient to approximate the action by a distribution $G(\Omega)$ of such harmonic oscillator potentials to simulate the loss of the kinetic energy of the electron to the lattice acquired as it falls through the impressed potential.[6] (One may recall that while neither a perfect inductor nor a perfect capacitor can dissipate energy, an infinite ladder of series inductors and shunt capacitors has a finite resistance.) We have not been able to find the corresponding variational principle, such as minimizing the free energy for a given expectation velocity, which would tell us the best possible distribution $G(\Omega)$ to use for a particular velocity. However, our expression for the field dependence of the velocity is relatively insensitive to the distribution. Thus while the determination of the actual distribution remains a very important unsolved problem, much of the physics of this problem is still open to us without explicit knowledge of $G(\Omega)$.

Thus let us set

$$\mathcal{I}_0 = \int_0^{t_2} \left(\tfrac{1}{2} m \dot{\bar{x}}^2(t) + \bar{F}(t)\cdot\bar{x}(t)\right) dt - \int_0^{t_2} \left(\tfrac{1}{2} m \dot{\bar{x}}'^2(t) + \bar{F}(t)\cdot\bar{x}'(t)\right) dt +$$

$$+ i \frac{\alpha A}{\sqrt{2}} \int_0^\infty G(\Omega)\, d\Omega \int_0^{t_2} dt \int_0^t dt' \Big[R_\Omega(t-t') \left(\bar{X}'(t) - \bar{X}'(t') \right)^2$$

$$+ R^*_\Omega(t-t') \left(\bar{X}(t) - \bar{X}(t') \right)^2 - R_\Omega(t-t') \left(\bar{X}(t) - \bar{X}'(t') \right)^2$$

$$- R^*_\Omega(t-t') \left(\bar{X}(t') - \bar{X}'(t) \right)^2 \Big] \,, \qquad (12)$$

and expand equation (9) as follows:

$$\int\int e^{i\Phi_e} = \int\int e^{i\Phi_o}\, e^{i(\Phi_e - \Phi_o)}$$

$$= \int\int e^{i\Phi_o} \left(1 + i(\Phi_e - \Phi_o) + \cdots \right) \qquad (13)$$

Notice that the various powers of $(\Phi_e - \Phi_o)$ include an electric field dependence only indirectly through $G(\Omega)$. The most sensitive dependence ($e^{i \bar{E}(t) \cdot \bar{X}(t)}$) is never altered.

While each term in the power series expansion (13) can be evaluated knowing the one basic path integral evaluated in the appendix, this approach would be algebraically unwieldy. We therefore make use of another argument, motivated in FHIP§4, which gives us a means to obtain what we believe to be a physically accurate estimate for the sum in (13).

Suppose for a moment we had a different problem, one in which the exact action Φ_1, was of the same form as that of Φ_o, except that the $G(\Omega)$ distribution of oscillator potentials was replaced by another distribution $H(\Omega)$. Then we could evaluate $\int\int e^{i\Phi_1}$ either exactly or by via the expansion (13):

$$\int\int e^{i\Phi_1} = \int\int e^{i\Phi_o}\, e^{i(\Phi_1 - \Phi_o)}$$

$$= \int\int e^{i\Phi_0}\,(1 + i(\Phi_1 - \Phi_0) + \cdots) \qquad (14)$$

It turns out that for our problem where we are interested only in the expectation value of the velocity in the limit $t_2 \to \infty$ (steady-state), that only the zero-order and first-order terms in (14) need be calculated in order to sum the series. (The other terms are not zero, however.)

To present this more clearly we refer to the following expansions:

$$\langle X(t_2)\rangle_e = \langle X(t_2)\rangle_0 + {}_e\langle X(t_2)\rangle_0 - {}_0\langle X(t_2)\rangle_0 + \cdots \qquad (15a)$$

$$\langle X(t_2)\rangle_1 = \langle X(t_2)\rangle_0 + {}_1\langle X(t_2)\rangle_0 - {}_0\langle X(t_2)\rangle_0 + \cdots \qquad (15b)$$

where

$${}_j\langle X(t_2)\rangle_K = \frac{1}{i}\Big|_{L=0} \frac{\partial}{\partial L} \int\int i\Phi_j\, e^{i\Phi_K}\, \mathcal{D}(\bar{X}(t))\, \mathcal{D}(\bar{X}'(t)) \qquad (15c)$$

$$\langle X(t_2)\rangle_K = \frac{1}{i}\Big|_{L=0} \frac{\partial}{\partial L} \int\int e^{i\Phi_K}\, \mathcal{D}(\bar{X}(t))\, \mathcal{D}(\bar{X}'(t)) \qquad (15d)$$

Also

$${}_jV_K = \lim_{t_2\to\infty} \frac{d}{dt_2}\, {}_j\langle X(t_2)\rangle_K \qquad (15e)$$

and

$$V_K = \lim_{t_2\to\infty} \frac{d}{dt_2} \langle X(t_2)\rangle_K \qquad (15f)$$

The v's represent the several velocities we must calculate. Upon evaluating the four terms in (15b) and determining (15e) and (15f) we find

$$\frac{1}{V_1} = \frac{1}{V_0} - \frac{{}_1V_0 - {}_0V_0}{V_0^2} \qquad (16)$$

to be an exact expansion of the velocity v_1. This is nothing more

than the first order expansion of the reciprocal of $v_1 \approx v_0 + (_1V_0 - {}_0V_0)$, as would be found from retaining only the first order terms in (15b). This correspondence, supplemented by the physical reasoning for using such expansions in this type of problem given in FHIP (p.1009), means that by setting

$$1/v_e = 1/v_0 - \frac{{}_eV_0 - {}_0V_0}{V_0^2} \tag{17}$$

we can obtain a far more accurate expression for v_e. The consistency between this approach and those of sections II and III is also reassuring. Also it turns out, moreover, that $1/v_0 = - {}_0V_0/V_0^2$ which reduces (17) to

$$v_e = - v_0^2/{}_eV_0 \tag{18}$$

This expression represents another step towards our E-V relationship.

D. The Evaluation of the Velocity

Once $\int\int e^{i\Phi_0}$ has been evaluated, various algebraic manipulations may be used to determine the v_0, ${}_ev_0$, and ${}_0v_0$ for equation (17). The calculation of this path integral is long and is outlined in the appendix. Using this result, we may at once find $\langle x(t_2)\rangle_0$ and $\langle x(t_2)\rangle_1$, for which $\bar{F}(t) = \hat{x}Eu(t) + \hat{x}L\delta(t - t_2^-)$ and $\bar{F}'(t) = \hat{x}Eu(t)$:

$$\langle X(t_2)\rangle_0 = -2E\,\mathrm{Im}\left(\int_0^{t_2} {}_GK_\beta(\tau)\,d\tau\right) \tag{19a}$$

$$\langle X(t_2)\rangle_1 = -2E\, \mathrm{Im}\left(\int_0^{t_2} {}_H K_\beta(\tau)\, d\tau\right) \qquad (19b)$$

where the pre-subscripts G and H refer to whether K_β was formed from the $G(\Omega)$ or $H(\Omega)$ oscillator distributions. Notice that

$$\mathrm{Im}\left(K_\beta(\tau)\right) = \int_0^\infty d\omega\, \Gamma(\omega)\, \sin\omega\tau \quad , \qquad (20)$$

which is independent of the temperature. It follows that

$$\langle \dot{X}(t_2)\rangle_0 = -2E\, \mathrm{Im}\, {}_G K_\beta(t_2) \qquad (21a)$$

and

$$\langle \dot{X}(t_2)\rangle_1 = -2E\, \mathrm{Im}\, {}_H K_\beta(t_2) \qquad (21b)$$

and passing to the limit $t_2 \to \infty$, we obtain

$$V_0 = \frac{E}{\pi\sqrt{2}\,\alpha(-A)\,g_1} \qquad (22a)$$

and

$$V_1 = \frac{E}{\pi\sqrt{2}\,\alpha(-A)\,h_1} \quad , \qquad (22b)$$

where $G(\Omega) = g_1\Omega + \cdots$ and $H(\Omega) = h_1\Omega + \cdots$, (Taylor series expansions of G and H about $\Omega = 0$, with $G(0) = H(0) = 0$). V_0 and V_1 are independent of the temperature and the electron mass.

These results express the fact that in zero order, where we consider merely the coupling of the electron to a lattice via a distribution of harmonic oscillator potentials in place of the more correct Coulomb interaction, the only oscillators capable of contributing to the D.C. mobility are those of lowest frequency. For

that problem (22a) and (22b) are exact for all values of electric field, and the relationship is linear as one would expect. (We remark in passing that a Hamiltonian H_o which leads to the action Φ_o in equation (12) is

$$H_o = \frac{\bar{p}^2}{2m} + \frac{1}{2}m\lambda^2\bar{x}^2 - \bar{F}(t)\cdot\bar{x} + \sum_{\bar{k}} \Omega_{\bar{k}}\, a_{\bar{k}}^{+} a_{\bar{k}} + \sum_{\bar{k}} \left(i D_{\bar{k}} a_{\bar{k}} (\bar{x}\cdot\bar{k}) - i D_{\bar{k}}^{*} a_{\bar{k}}^{+} (\bar{x}\cdot\bar{k}) \right)$$

where $$m\lambda^2 = \frac{8\alpha(-A)}{\sqrt{\pi}} \int_0^\infty d\Omega\, \frac{G(\Omega)}{\Omega} = \int \frac{d^3k}{(2\pi)^3} |D_{\bar{k}}|^2 \frac{k^2}{3} \frac{1}{\Omega_{\bar{k}}} \quad ,$$

in which the linear coupling to the oscillators is explicitly apparent. But because this Hamiltonian no longer represents the non-linearities inherent in the original problem, we do <u>not</u> use H_o here.)

In order to calculate $\langle x(t_2)\rangle_o$ and $\langle x(t_2)\rangle_o$ we must perform $\int\int e^{i\Phi_o}\, i\Phi_o$ and $\int\int e^{i\Phi_o}\, i\Phi_1$. In fact, the former can be obtained from the latter by replacing $H(\Omega)$ by $G(\Omega)$. Also, as it is only the difference of actions $(\Phi_1 - \Phi_o)$ which enters, we need consider only the third term in (12). As a shorter notation, we designate the solution of $\int\int e^{i\Phi_o}$ by $\int\int \{\bar{F}(t), \bar{F}'(t)\}$ where we specify the forces to be inserted into $\int\int e^{i\Phi_o}$. Using this notation we may write

$$\int\int e^{i\Phi_o}\, i\Phi_1 = -\frac{\alpha(-A)}{\sqrt{\pi}} \int_0^\infty H(\Omega)\, d\Omega \int_{-\infty}^{\infty} d\theta \int_{-\infty}^{\theta} d\eta \left[R_\Omega(\theta-\eta)\Big|_{\bar{K}=0} \frac{d^2}{d\bar{K}^2}\left(\int\int(1)\right) \right.$$

$$\left. + R_\Omega^{*}(\theta-\eta)\Big|_{\bar{K}=0} \frac{d^2}{d\bar{K}^2}\left(\int\int(2)\right) - R_\Omega(\theta-\eta)\Big|_{\bar{K}=0} \frac{d^2}{d\bar{K}^2}\left(\int\int(3)\right) - R_\Omega^{*}(\theta-\eta)\Big|_{\bar{K}=0} \frac{d^2}{d\bar{K}^2}\left(\int\int(4)\right) \right] \tag{23}$$

where $$\frac{d^2}{d\bar{K}^2} = \frac{d^2}{dk_x^2} + \frac{d^2}{dk_y^2} + \frac{d^2}{dk_z^2} \tag{23a}$$

and

$$\left.\begin{aligned}
&\iint(1)=\iint\{\bar{F}(t)=(Eu(t)+L\delta(t-t_2^-))\hat{x}\,,\ \bar{F}'(t)=Eu(t)\hat{x}+\bar{k}(\delta(t-\theta)-\delta(t-\eta))\}\\
&\iint(2)=\iint\{\bar{F}(t)=(Eu(t)+L\delta(t-t_2^-))\hat{x}+\bar{k}(\delta(t-\theta)-\delta(t-\eta))\,,\ \bar{F}'(t)=Eu(t)\hat{x}\}\\
&\iint(3)=\iint\{\bar{F}(t)=(Eu(t)+L\delta(t-t_2^-))\hat{x}+\bar{k}\delta(t-\theta)\,,\ \bar{F}'(t)=Eu(t)\hat{x}+\bar{k}\delta(t-\eta)\}\\
&\iint(4)=\iint\{\bar{F}(t)=(Eu(t)+L\delta(t-t_2^-))\hat{x}+\bar{k}\delta(t-\eta)\,,\ \bar{F}'(t)=Eu(t)\hat{x}+\bar{k}\delta(t-\theta)\}
\end{aligned}\right\}\quad(23b)$$

Although the algebra is quite involved, the results are quite simply expressible:

$$ {}_0V_0 = -\frac{E g_1}{\pi\sqrt{2}\,\alpha(-A)\,g_1^2} \qquad (24a)$$

$$ {}_1V_0 = -\frac{E h_1}{\pi\sqrt{2}\,\alpha(-A)\,g_1^2} \qquad (24b)$$

Again there is no temperature or mass dependence. Note also that ${}_1V_0 = -{}_0V_0/V_0^2$, which is needed to reduce (17) to (18).

The calculation of $\iint i\mathcal{I}_e\, e^{i\Phi_0}$ to obtain ${}_eV_0$ can be performed using

$$\iint i\mathcal{I}_e e^{i\Phi_0} = -\int\frac{d^3k}{(2\pi)^3}|C_k|^2\int_{-\infty}^{\infty}d\theta\int_{-\infty}^{\theta}d\eta\,[R_{\omega_{\bar{k}}}(\theta-\eta)\iint(1)$$

$$+R^*_{\omega_{\bar{k}}}(\theta-\eta)\iint(2)-R_{\omega_{\bar{k}}}(\theta-\eta)\iint(3)-R^*_{\omega_{\bar{k}}}(\theta-\eta)\iint(4)] \qquad (25)$$

where the notation of (23b) applies. Again doing the algebra and inserting the result for ${}_eV_0$ into (18) yields

$$\frac{1}{v_e} = -\frac{1}{v_o^2}\left(-\frac{v_o}{E}\int_{-\infty}^{\infty} d\xi \int \frac{d^3K}{(2\pi)^3} |C_{\bar{k}}|^2 k_x R_{w_{\bar{k}}}(\xi)\, e^{-ik_x \xi v_o}\, e^{-K^2 \bar{K}_\beta(\xi)}\right) \quad (26)$$

where $$\bar{K}_\beta(\xi) = \int_0^\infty dw \,(-\Gamma'(w))\left(\frac{1-e^{iw\xi}}{1-e^{-\beta w}} + \frac{1-e^{-iw\xi}}{e^{\beta w}-1}\right) \quad (26a)$$

E. The Electric Field-Velocity Relationship

The result obtained in (26) for the approximate velocity v_e as a function of E, the electric field, is unsatisfactory in one respect: the critical dependence through v_o of the result on the particular oscillator distribution for small Ω . To remedy this we are motivated to replace v_o and v_e in (26) by v, the expectation, steady-state velocity. The result is

$$E = \int_{-\infty}^{\infty} d\xi \int \frac{d^3K}{(2\pi)^3} |C_{\bar{k}}|^2 k_x R_{w_{\bar{k}}}(\xi) e^{-ik_x \xi v}\, e^{-K^2 \bar{K}_\beta(\xi)} \,, \quad (27)$$

as our fundamental equation relating the velocity to the electric field. Several excellent reasons for this replacement are presented in the next and following sections; they are based on an examination of several other computations in different limits of velocity, coupling, and temperature. Equation (27) includes the nonlinearities of the problem: it is just that they are not included precisely.

III. Comparison with Other Results.

In this section we compare our equation (27) for E versus v with several other relationships to demonstrate that this equation includes the physical effects we would expect from the nature of the problem.

A. Comparison with Equation (26)

As may be seen by inspection, in the limit of low velocities, where we may expand $e^{-ik_x \xi v_0}$ in (26) and $e^{-ik_x \xi v}$ in (27) in power series and identify v with v_e, the equations agree. This comparison is valid for arbitrary coupling and arbitrary temperature.

B. Comparison with Weak Coupling Model

If we consider the special case of the electron in the crystal lattice under the hypothesis that the interaction is so weak that we may consider the collisions with optical phonons to occur essentially independently, that is, sufficiently separated in time that quantum interferences among these collisions are negligible, then using first order perturbation theory (Fermi's Golden Rule), we can determine the net rate at which the electron loses momentum. In steady state this rate just equals the applied force, in this case the electric field.

The rate at which the electron loses momentum $\bar{k}$ in a lattice at thermal equilibrium is $2\pi |C_{\bar{k}}|^2 \delta\left(-\frac{K^2}{2m} + \frac{\bar{p}_i \cdot \bar{k}}{m} - \omega_{\bar{k}}\right) / \left(1 - e^{-\beta \omega_{\bar{k}}}\right)$, and the rate at which it acquires momentum $\bar{k}$ is

$2\pi |C_{\bar{k}}|^2 \delta(-\frac{k^2}{2m} - \frac{\bar{p}_i \cdot \bar{k}}{m} + \omega_{\bar{k}})/(e^{\omega_{\bar{k}}\beta} - 1)$, where $\bar{p}_i$ is the momentum of the electron before the collision. Replacing the delta function by $2\pi\delta(x) = \int_{-\infty}^{\infty} e^{-ix\xi}\, d\xi$, summing over all possible $\bar{k}$, and averaging $\bar{p}_i$ over a Maxwell-Boltzmann distribution of electrons with mean velocity v in the direction of E, we obtain for the equation expressing the conservation of momentum in the $\hat{x}$ direction ($\bar{E} \parallel \hat{x}$),

$$E = \int_{-\infty}^{\infty} d\xi \int \frac{d^3k}{(2\pi)^3} |C_{\bar{k}}|^2 k_x \left(\frac{e^{i\omega_{\bar{k}}\xi}}{1 - e^{-\omega_{\bar{k}}\beta}} + \frac{e^{-i\omega_{\bar{k}}\xi}}{e^{\beta\omega_{\bar{k}}} - 1} \right) e^{-ik_x v \xi} e^{-k^2 \bar{K}_\beta'(\xi)} \tag{28}$$

where $\bar{K}'_\beta(\xi) = \frac{1}{2}\left(\xi^2/\beta - i\,\xi/m \right)$. From FHIP we recall that for low α ($\alpha < 1$) one uses for $\mathcal{F}_0$ just the free-electron influence functional which gives $\bar{K}_\beta(s) = \frac{1}{2}\left(s^2/\beta - i\,s/m \right)$ in (27). Again we obtain a consistent correspondence as well as a hint as to how to go about solving our problem more quickly. This hint is exploited in section IV. Of course, in order to assume a Maxwell-Boltzmann distribution as we do, we must assume that for a given velocity the temperature is sufficiently large so that $1/2mv^2 \ll kT$ is satisfied.

C. Comparison with Rate of Energy Transfer

One may calculate to lowest order the rate at which energy is being transferred from the electron to the lattice using the expression

$$W_o = \lim_{t_2 \to \infty} \frac{d}{dt}\, Tr\left(\sum_{\bar{k}} \omega_{\bar{k}} a^+_{\bar{k}} a_{\bar{k}}\, \rho \right) \tag{29}$$

in a manner similar to that used to calculate Tr(xρ). The result is

$$W_o = \int_{-\infty}^{\infty} d\xi \int \frac{d^3k}{(2\pi)^3} \omega_{\bar{k}} |C_{\bar{k}}|^2 \left(\frac{e^{i\omega_{\bar{k}}\xi}}{1-e^{-\beta\omega_{\bar{k}}}} - \frac{e^{-i\omega_{\bar{k}}\xi}}{e^{\beta\omega_{\bar{k}}}-1} \right) e^{-ikv_o\xi} e^{-k^2\bar{K}_\beta(\xi)} \quad (30)$$

Again replacing v_o by v we obtain a more physically accurate result. This is evident for weak coupling by carrying out section B for rate of energy loss. The result is equation (30) with v_o replaced by v and $\bar{K}_\beta(\xi)$ replaced by the free electron $\bar{K}'_\beta(\xi)$. Thus again from the weakly coupled problem we obtain the essential form of the velocity dependence and from the arbitrarily coupled problem, the form of $\bar{K}_\beta(\xi)$, which corresponds to a scattering probability (FHIP p. 1011).

(In principle one should be justified in writing $W_o = Ev$, expressing the fact that the rate at which the electron loses energy must equal the expected value of the force times the velocity, and this result could be compared with the E-v relation of section B (28) or (27). If both results were precise, they would, of course, be equivalent. By the result of the approach used in § II to obtain (27), we regard the momentum relation to be the more accurate of the two. However, both relationships give quite similar physical behavior. We discuss this further in § IV.)

IV. Second Approach - - The Method of Rates

In sections B and C of the last article, the conservation of the energy and momentum in the steady state was utilized in finding relationships between electric field and velocity for weak coupling. In this article we formulate this procedure in a general manner. This will have the advantage of eliminating the necessity of having to take time derivatives, as well as casting the result directly into the form of (27).

The time rate of loss of the electron momentum and the time rate of loss of electron energy are given by

$$Tr\left(\frac{d}{dt}\left(\sum_{\bar{k}} \bar{k}\, a_{\bar{k}}^{+} a_{\bar{k}}\right)\rho\right) \tag{31}$$

and

$$Tr\left(\frac{d}{dt}\left(\sum_{\bar{k}} w_{\bar{k}}\, a_{\bar{k}}^{+} a_{\bar{k}}\right)\rho\right) \tag{32}$$

respectively. The time derivatives are easily computed from $i\hbar \dot{O} = [O, H]$, and, if we define

$$\hat{R}_{\bar{k}} = -i\left(C_{\bar{k}}^{*}\, a_{\bar{k}}^{+} e^{-i\bar{k}\cdot\bar{x}} - C_{\bar{k}}\, a_{\bar{k}} e^{i\bar{k}\cdot\bar{x}}\right) \quad , \tag{33}$$

then (31) and (32) become

$$Tr\left(\sum_{\bar{k}} \hat{R}_{\bar{k}}\, \bar{k}\, \rho(t)\right) = \sum_{\bar{k}} \bar{k}\, Tr\left(\hat{R}_{\bar{k}}\, \rho(t)\right) \tag{31a}$$

$$Tr\left(\sum_{\bar{k}} \hat{R}_{\bar{k}}\, w_{\bar{k}}\, \rho(t)\right) = \sum_{\bar{k}} w_{\bar{k}}\, Tr\left(\hat{R}_{\bar{k}}\, \rho(t)\right) \tag{32a}$$

The expression $\mathrm{Tr}(\hat{R}_k \rho(t))$ gives the net rate of production of phonons of momentum $\bar{k}$ at time t. Such a quantity is useful not only in calculating the electric field-velocity relationship, but also, for instance, in determining the angular dependence of the phonon energy emitted from the polaron "shock wave" for velocities above the "critical velocity for the emission of optical phonons." (This latter comment refers to the second order perturbation theory result for the polaron energy. For electron momentum above $\sqrt{2}$ (electron energy greater than $\omega_k = 1$) this energy becomes complex, and twice its imaginary part is the approximate rate at which phonons are emitted.)

We again use equation (3) to substitute for $\rho(t)$, eliminate the oscillator coordinates, and transform the result into a double path integral to obtain

$$R_{\bar{k}} = \mathrm{Tr}\left(\hat{R}_{\bar{k}}\, \rho(t_2)\right) = |C_{\bar{k}}|^2 \iint e^{i\mathcal{F}_e} \int_0^{t_2} dt \left\{ \frac{e^{i\bar{k}\cdot(\bar{x}_{t_2}-\bar{x}_t)}\, e^{-i\omega_{\bar{k}}(t_2-t)}}{1-e^{-\beta\omega_{\bar{k}}}} - \frac{e^{-i\bar{k}\cdot(\bar{x}_{t_2}-\bar{x}_t)}\, e^{i\omega_{\bar{k}}(t_2-t)}}{e^{\beta\omega_{\bar{k}}}-1} + \frac{e^{-i\bar{k}\cdot(\bar{x}_{t_2}-\bar{x}'_t)}\, e^{i\omega_{\bar{k}}(t_2-t)}}{1-e^{-\beta\omega_{\bar{k}}}} - \frac{e^{i\bar{k}\cdot(\bar{x}_{t_2}-\bar{x}'_t)}\, e^{-i\omega_{\bar{k}}(t_2-t)}}{e^{\beta\omega_{\bar{k}}}-1} \right\} \mathcal{D}(x(t))\,\mathcal{D}(x'(t)) \qquad (34)$$

where $\mathcal{F}_e$ is given in equation (10). At this point we could use momentum conservation to give $E = \sum_{\bar{k}} k_x R_k$. This equation also follows immediately from $\partial/\partial x_{t_2}\left(\iint e^{i\mathcal{F}_e}\right) = 0$: $\iint e^{i\mathcal{F}_e}$ is independent of x_{t_2} since the path integral is integrated over x_{t_2}.

However, as we shall see, a more physical approach is to change the variables of integration in (34) to $\bar{x} = \bar{y} + \bar{v}t$ and $\bar{x}' = \bar{y}' + \bar{v}t$, where v is the expectation velocity of the electron, to obtain

$$R_{\bar{k}} = |C_{\bar{k}}|^2 \int_0^{t_2} d\xi \iint e^{i\Phi_e'} \left\{ \frac{e^{-i\omega_{\bar{k}}'(t_2-\xi)}}{1-e^{-\beta\omega_{\bar{k}}}} e^{i\bar{k}\cdot(\bar{y}_{t_2}-\bar{y}_\xi)} - \frac{e^{i\omega_{\bar{k}}'(t_2-\xi)} e^{-i\bar{k}\cdot(\bar{y}_{t_2}-\bar{y}_\xi)}}{e^{\beta\omega_{\bar{k}}}-1} \right.$$

$$\left. + \frac{e^{i\omega_{\bar{k}}'(t_2-\xi)} e^{-i\bar{k}\cdot(\bar{y}_{t_2}-\bar{y}_\xi')}}{1-e^{-\beta\omega_{\bar{k}}}} - \frac{e^{-i\omega_{\bar{k}}'(t_2-\xi)} e^{i\bar{k}\cdot(\bar{y}_{t_2}-\bar{y}_\xi')}}{e^{\beta\omega_{\bar{k}}}-1} \right\} \mathcal{D}(\bar{y}(t)) \mathcal{D}(\bar{y}'(t)) \quad (35)$$

where

$$\Phi_e' = \int_0^{t_2} \left(\frac{m\dot{\bar{y}}^2}{2} + \bar{F}(t)\cdot\bar{y} \right) dt - \int_0^{t_2} \left(\frac{m\dot{\bar{y}}'^2}{2} + \bar{F}'(t)\cdot\bar{y}' \right) dt$$

$$+ i \int \frac{d^3k}{(2\pi)^3} |C_{\bar{k}}|^2 \int_0^{t_2} dt \int_0^{t} dt' \left(S_{\omega_{\bar{k}}'}(t-t')\, e^{-i\bar{k}\cdot(\bar{y}_t'-\bar{y}_{t'}')} + S_{\omega_{\bar{k}}'}^*(t-t') e^{i\bar{k}\cdot(\bar{y}_t-\bar{y}_{t'}')} \right.$$

$$\left. - S_{\omega_{\bar{k}}'}(t-t') e^{-i\bar{k}\cdot(\bar{y}_t-\bar{y}_{t'}')} - S_{\omega_{\bar{k}}'}^*(t-t') e^{-i\bar{k}\cdot(\bar{y}_t'-\bar{y}_{t'})} \right), \quad (35a)$$

$$S_{\omega_{\bar{k}}'}(\tau) = \frac{e^{i\omega_{\bar{k}}'\tau}}{1-e^{-\beta\omega_{\bar{k}}}} + \frac{e^{-i\omega_{\bar{k}}'\tau}}{e^{\beta\omega_{\bar{k}}}-1}, \quad (35b)$$

and $$\omega_{\bar{k}}' = \omega_{\bar{k}} - k_x v \quad (35c)$$

Again to proceed farther, we must approximate the action Φ_e' so that the path integrals can be performed, but without loss of the essential physics. Only now that we are in a system translating with the electron, the replacement of the actual electrostatic interaction by parabolic potentials centered in the mean position of the electron should permit a more accurate determination of $\bar{K}_\beta(\xi)$.

In particular, $\bar{K}_\beta(\xi)$ will have velocity dependence in addition to that through $G(\Omega)$, the oscillator distribution. The computation of this improved approximation is quite involved; the result has only a small additional dependence on the velocity and offers little further insight into the problem. This further supports the statement that $\bar{K}_\beta(\xi)$ is relatively insensitive to the velocity.

If we formulate the result for R_k in terms of the model of § II, we obtain

$$R_{\bar{k}} = |C_{\bar{k}}|^2 \int_0^{t_2} dt \left\{ \left(\frac{e^{i(\omega_{\bar{k}} - k_x v)t}}{1 - e^{-\beta\omega_{\bar{k}}}} - \frac{e^{-i(\omega_{\bar{k}} - k_x v)t}}{e^{\beta\omega_{\bar{k}}} - 1} \right) e^{-k^2 \bar{K}_\beta(t)} \right.$$

$$\left. + \left(\frac{e^{-i(\omega_{\bar{k}} - k_x v)t}}{1 - e^{-\beta\omega_{\bar{k}}}} - \frac{e^{i(\omega_{\bar{k}} - k_x v)t}}{e^{\beta\omega_{\bar{k}}} - 1} \right) e^{-k^2 \bar{K}_\beta^*(t)} \right\}$$

$$= |C_{\bar{k}}|^2 \int_{-t_2}^{t_2} dt \left\{ \frac{e^{i(\omega_{\bar{k}} - k_x v)t}}{1 - e^{-\beta\omega_{\bar{k}}}} - \frac{e^{-i(\omega_{\bar{k}} - k_x v)t}}{e^{\beta\omega_{\bar{k}}} - 1} \right\} e^{-k^2 \bar{K}_\beta(t)} \quad (36)$$

and if we let $t_2 \to \infty$ for steady state, we recover our basic E-v relation (27) from $E = \sum_{\bar{k}} k_x R_{\bar{k}}$. Using $W = \sum_{\bar{k}} \omega_{\bar{k}} R_{\bar{k}}$, we also obtain approximately the rate at which energy is being transferred from the electron to the optical vibrations of the crystal, as discussed in § III. C. Physically this quantity must equal the product of the field and the expectation velocity (Ev), which also gives an E-v relation. One might be tempted to argue that we should constrain our oscillator distribution to be such that the two E-v relations agree identically. But then another calculation with the $R_{\bar{k}}$ would not have the accuracy one might claim on the basis of such agreement. We prefer to regard (27) as our final expression, and use greater care in

applying the approximate rate, $R_{\tilde{k}}$.

V. Note Regarding a Variational Principle

The most natural variational method to try would be to extend Feynman's approach in reference (1) to our distribution of oscillators at finite temperature. The result is

$$F_e \leq \frac{3}{\beta}\sum_{n=1}^{\infty} \ln\left(\frac{\bar{Z}(\omega_n)}{m\omega_n^2}\right) - \frac{3}{\beta}\sum_{n=1}^{\infty}\left(1-\frac{m\omega_n^2}{\bar{Z}(\omega_n)}\right)$$

$$-\int_0^\beta d\xi \int \frac{d^3\bar{k}}{(2\pi)^3}|C_{\bar{k}}|^2\left(\frac{e^{-\omega_{\bar{k}}\xi}}{1-e^{-\beta\omega_{\bar{k}}}}+\frac{e^{\omega_{\bar{k}}\xi}}{e^{\omega_{\bar{k}}\beta}-1}\right)e^{-\frac{2}{\beta}k^2\Sigma} \qquad (37)$$

where $$\Sigma = \sum_{n=1}^{\infty}\frac{1}{\bar{Z}(\omega_n)}(1-\cos\omega_n\xi) \qquad (37a)$$

and $$\bar{Z}(\omega_n) = m\omega_n^2 + \frac{8\alpha(-A)}{\sqrt{\beta^7}}\int_0^\infty \frac{G(\Omega)\,\omega_n^2}{\Omega(\Omega^2+\omega_n^2)}\,d\Omega \qquad (37b)$$

(Note $Z(\nu) = -\bar{Z}(-i(\nu + i\epsilon))$: see (A-14).) This inequality tells us that if we choose the $\bar{Z}(\omega_n)$, $n = 1, 2, \ldots$, so that F_e is as small as possible, then the corresponding oscillator distribution $G(\Omega)$, or for that matter the corresponding $Z(\nu)$, which is all we need, is the distribution to be used in computing $\bar{K}_\beta(\xi)$. However, if we write $\bar{K}_\beta(\xi)$ (26a) in the equivalent form

$$\bar{K}_\beta(\xi) = -\int_{-\infty}^{\infty}\frac{d\omega}{2\pi i}\,\frac{1}{Z(\omega)}\left(\frac{1-e^{i\omega\xi}}{1-e^{-\beta\omega}}+\frac{1-e^{-i\omega\xi}}{e^{\beta\omega}-1}\right) \qquad (38)$$

and recall all poles and zeroes of $Z(\omega)$ lie in the lower half plane, then we see that knowing $Z(\omega)$ only at $\omega = i\omega_n$ is insufficient to

determine $\bar{K}_\beta(\xi)$. To be sure one can still introduce a distribution of oscillators which depends on only a few parameters and minimize (37) with respect to each to obtain the value of these parameters. But the problem of determining a variational principle for processes similar to the polaron one considered here is much harder and deeper than this.

VI. Numerical Results

The crucial test of our E-v relationship is, in the absence of experimental data, physical reality. Taking for our distribution of oscillators, a single oscillator, just as was used in references (1) and (2), choosing for the frequency and oscillator strength parameters those values giving the lowest free energy at zero temperature,[1, 2] using the Frȍhlich Hamiltonian, and assuming $\omega_{\bar{k}} = 1$ for all $\bar{k}$, we present the electric field versus velocity for couplings of $\alpha = 3$ and $\alpha = 7$, for β's between 20 and .001. In our units β is the ratio of the energy of the longitudinal optical mode to the average thermal energy of the lattice. Typical longitudinal reststrahl energies range between room temperature and six times room temperature. (The longitudinal reststrahl can be determined from the experimentally measured transverse reststrahl frequency using $\omega_L/\omega_T = \sqrt{\epsilon/\epsilon_\infty}$[9] where ϵ is the D.C. dielectric constant and ϵ_∞ is the electronic contribution to the dielectric constant.)

For numerical work it is convenient to cast the integrand of (27) into a purely real form. In general, $\bar{K}_\beta(\xi)$ is positive and otherwise well-behaved in the region $-\infty \le Re(\xi) \le \infty$, $0 \le Im(\xi) \le \beta$. If we shift the contour from $Im(\xi) = 0$ to $Im(\xi) = \beta/2$, we obtain

$$E = \int_{-\infty}^{\infty} d\xi \int \frac{d^3K}{(2\pi)^3} |C_{\bar{K}}|^2 k_x \frac{\cos \omega_K \xi}{\sinh \omega_K \beta/2} e^{-ik_x v(\xi + i\beta/2)} e^{-k^2 \bar{\bar{K}}_\beta(\xi)} \quad (39)$$

where $$\bar{\bar{K}}_\beta(\xi) = \int_0^\infty d\omega (-\Gamma(\omega)) \left(\tanh \frac{\beta\omega}{4} + \frac{1 - \cos \omega \xi}{\sinh \beta\omega/2} \right) \quad (39a)$$

(Only the real part of $e^{-iK_x v(\xi + i\beta/2)}$ enters, of course, but (39) is a just-as-good place to start.) Making the substitutions indicated in the first paragraph, we find

$$E = \frac{4\alpha}{v^2 \beta \sqrt{\pi}\, \sinh \beta/2} \int_0^{v\sqrt{\beta}\frac{v_0}{w_0}} x^2 dx \int_0^\infty ds \frac{\cos \frac{\beta s}{2}}{A(s)^{3/2}} e^{-x^2 \frac{s^2-1}{2A(s)}} \left(\cos \frac{x^2 s}{A(s)} - s \cdot \sin \frac{x^2 s}{A(s)} \right) \quad (40)$$

where

$$A(s) = s^2 + 1 + \frac{4}{\beta} \frac{v_0^2 - w_0^2}{w_0^2 v_0} \frac{\cosh \beta v_0/2 - \cos s v_0 \beta/2}{\sinh \beta v_0/2} \quad (40a)$$

and w_0 and v_0 are the variational parameters corresponding to α. The values used here are $\alpha = 3$, $v_0 = 3.4$, $w_0 = 2.5$, and $\alpha = 7$, $v_0 = 5.8$, $w_0 = 1.6$. (FHIP p. 1012.) While one would expect these values to be valid only for large β (low temperature), we use them for all temperatures. In fact for high temperatures ($\beta > 0.1$) the E-v relation no longer depends significantly on w_0, v_0. This is seen by expanding A(s) for small β: $A(s) \approx (v_0^2 / w_0^2)(s^2 + 1)$, and setting $z = (w_0 / v_0)x$ in the first integral. Therefore, we expect the numerical results to be about as good as would be obtained if different v_0, w_0 were inserted at each temperature.

The results of the computer work are shown in figures 1 and 2. For $\beta \geq 5.0$, the linear region was also calculated by hand. The variables shown (EE, vv) are related to the dimensionless variables (E, v) used above by the equalities

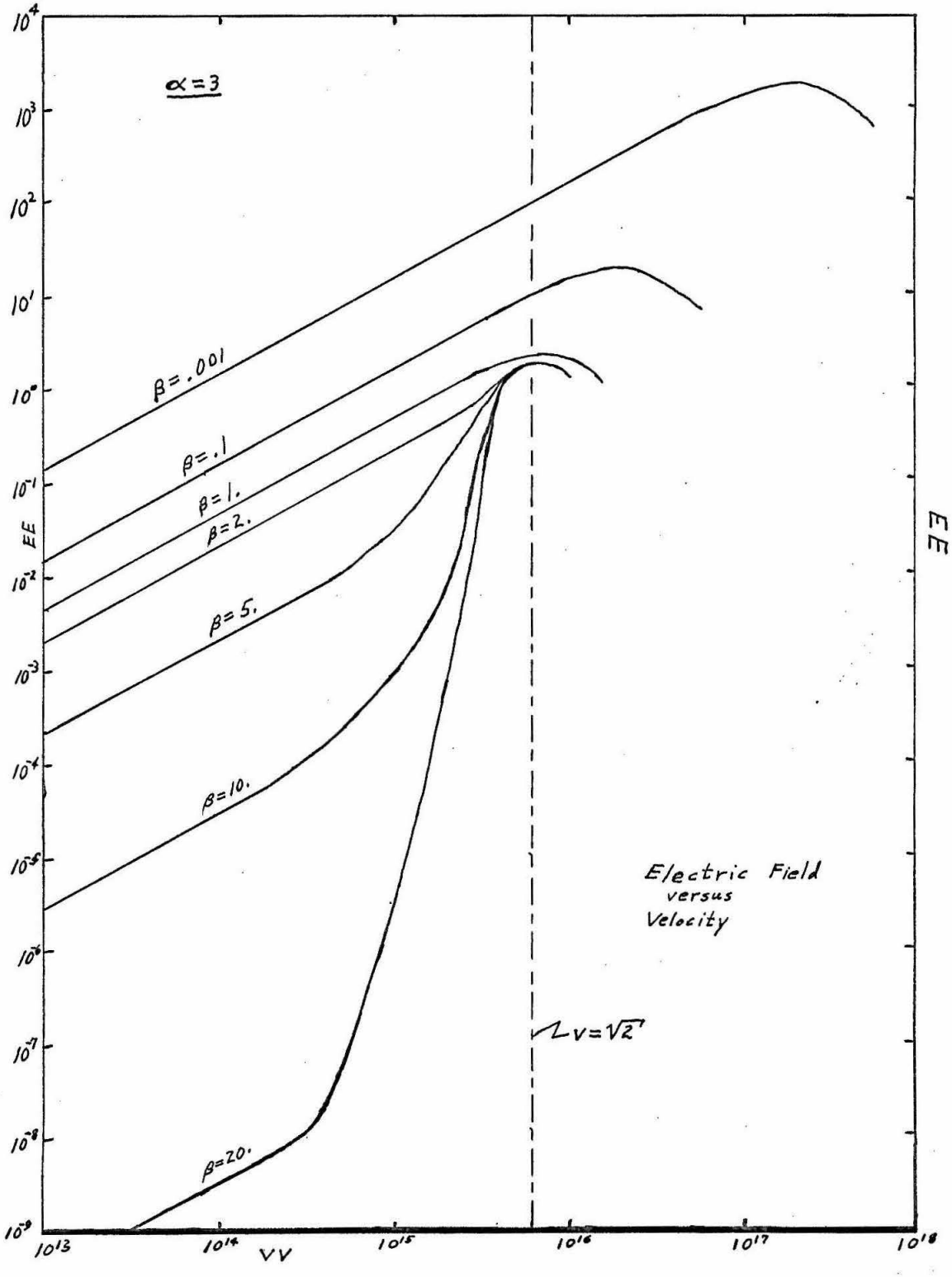
α=3
β=.001
β=.1
β=1.
β=2.
β=5.
β=10.
β=20.
EE
EE
VV
V=√2
Electric Field
versus
Velocity
10^4
10^3
10^2
10^1
10^0
10^-1
10^-2
10^-3
10^-4
10^-5
10^-6
10^-7
10^-8
10^-9
10^13
10^14
10^15
10^16
10^17
10^18

Figure 1

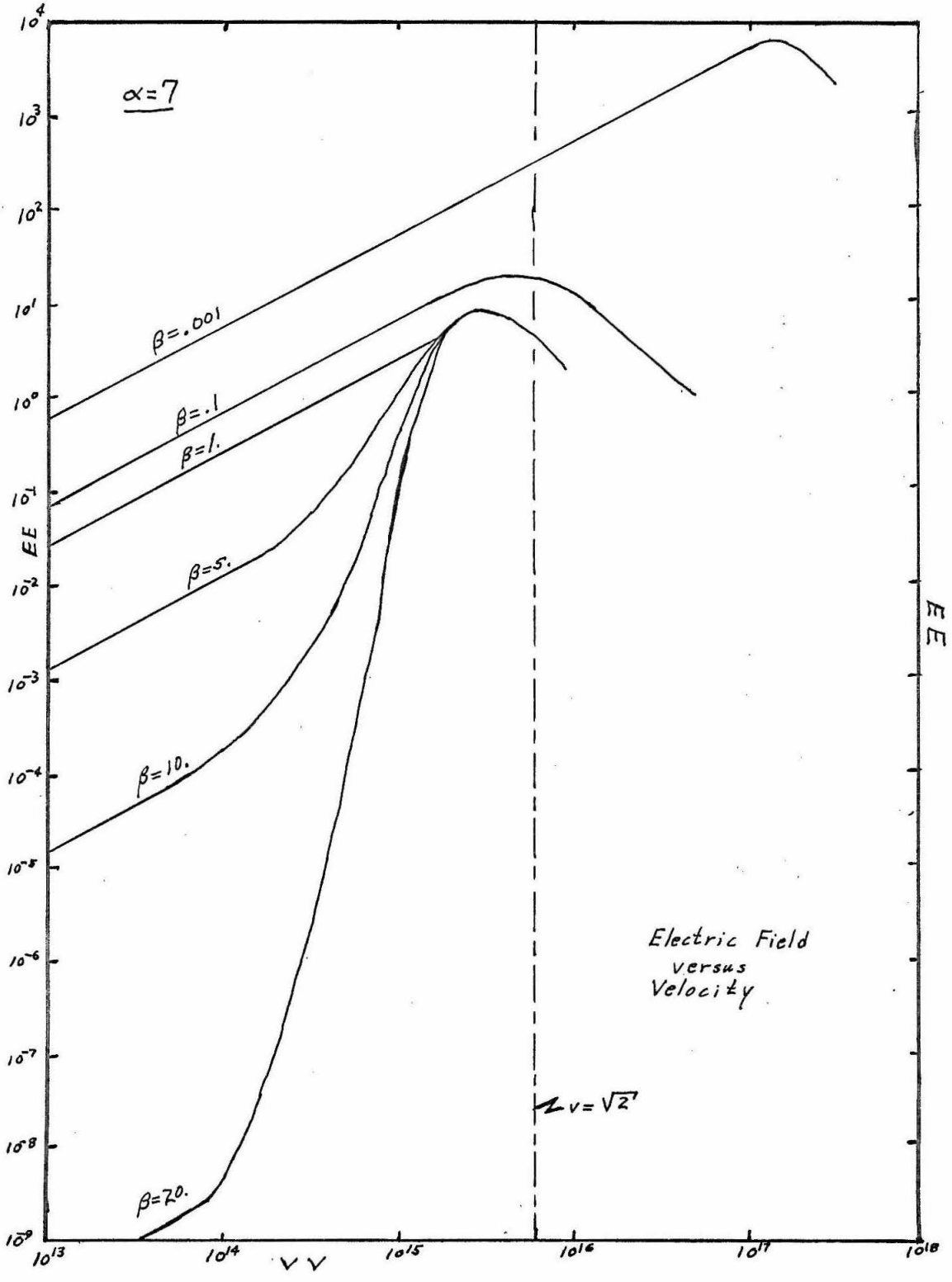
α=7
β=.001
β=.1
β=1.
β=5.
β=10.
β=20.
EE
VV
V=√2
Electric Field
versus
Velocity

Figure 2

$$VV = v \cdot \frac{1}{\sqrt{m_e}} \approx v \cdot .418 \cdot 10^{16} \qquad (41a)$$

$$EE = E \cdot \frac{\sqrt{m_e}}{\hbar} \approx E \cdot 2.75^{-1} \qquad (41b)$$

where m_e is the mass of the electron in eV-sec^2/Å^2. To obtain eE, the force on the electron in eV/Å, and v_r, the velocity in Å/sec, one uses

$$v_r = \sqrt{\frac{m_e}{m^*}} \cdot \sqrt{\hbar\omega_L} \cdot VV \quad (Å/sec) \qquad (42a)$$

$$eE = \sqrt{\frac{m^*}{m_e}} \, (\hbar\omega_L)^{3/2} \cdot EE \quad (eV/Å) \qquad (42b)$$

where m^* is the fixed-lattice, effective mass, and $\hbar\omega_L$ is expressed in eV.

The physical interpretation of the curves is straightforward. For $\beta \geq 2.0$, about room temperature and below, the field-velocity relation is linear until the translational kinetic energy of the electron approaches the reststrahl energy (vertical dashed line). Then the electric field must be increased to a threshold approximately independent of temperature before the velocity of the electron can again be increased substantially. However, once the threshold is reached, further increases in the electric field appear to no longer correspond to physical velocities. This means that beyond the threshold of the electric field, the electron is effectively "pulled out" of the polaron state, and other mechanisms, such as

acoustic phonon scattering, impurity scattering, etc., must be included in the physics of the problem to limit the electron's acceleration. For higher temperatures, $\beta < 2.0$, the effect is less dramatic. However now the threshold for breaking out of the polaron state increases with temperature, as does the velocity where this occurs. This is evident physically if we recall that for only $\beta \lesssim 2.0$ do we have appreciable numbers of optical phonons in the crystal, and as the temperature increases further, this number increases rapidly. Thus the electron encounters far more scattering from phonons already present, and consequently higher and higher fields are required to overcome this damping.

Let us consider, as a specific example, the case of MgO: $\alpha \simeq 3$; assume $\sqrt{\frac{m^*}{m_e}} \approx 1$; $\hbar\omega_L = .0730\sqrt{9.65/3.03} = .13\text{eV}$.[10] Then the threshold field for temperatures $\lesssim 750^\circ\text{K}$ ($\beta=2$) is about .1 eV/Å . Thus on the basis of this theory, we would predict that in order to accelerate an electron in MgO to energies of over .13eV, an electric field strength of about .1eV/Å (10^7 volts/cm) is necessary. This may be a relevant minimum voltage for the operation of cold electron emission devices using MgO as the insulator.[11, 12] The threshold for exceeding the reststrahl energy for Al_2O_3 will lie higher by about a factor of 2, and that for BeO, lower by about the same factor.

VII. Conclusions.

In this paper we have treated the motion of an electron in a polarizable crystal under the influence of a D.C. electric field. Starting with the crystal in thermal dynamic equilibrium, the electron was injected with zero velocity, and its subsequent steady-state motion was determined using two methods. In one approach the expectation value of displacement of the electron was found, and the time derivative gave the steady-state velocity. In the other approach, the rate of loss of electron momentum to the lattice was set equal to the electric field to obtain the E-v relationship. In both cases no approximation regarding the field strength, velocity, lattice coupling constant, or temperature was ever made. However, the part of the action in the Feynman Path Integral related to the electron-lattice interaction is approximated as closely as possible to physical reality, and expansions in the difference of the exact and approximate actions are combined in manners suggested by the exact solution of similar problems. The resulting expression relating E, the electric field, to v, the velocity of the electron, is an explicit formula for E as a function of v, and was evaluated numerically over a temperature range of $2 \cdot 10^5$ for two coupling constants. The results give physically reasonable thresholds for the electric field strengths necessary to "pop" the electron out of the polaron, which may be at the root of the current problem of the low yield in tunnel-emission devices. They also exhibit the qualitatively expected features of E-v curves in β below threshold.

Appendix - - The Calculation of the Path Integral

In this section we outline the calculation of

$$\mathcal{J} = \int\int e^{i\mathcal{F}_0} \mathcal{D}(\bar{x}(t)) \mathcal{D}(\bar{x}'(t)) \qquad (A-1)$$

where $\mathcal{F}_0$ is given by equation (12). In order to avoid the usual problems which arise in performing path integrals over finite intervals with complex exponents (especially the presence of undamped transcients), we change the limits of the time integrals from $\int_0^{t_2}$ to $\int_{-\infty}^{\infty}$, while at the same time changing F(t) and F'(t) appropriately to ensure that physically we are still working with the same problem. To facilitate this transition, we recall that the path integral may be interpreted as a kernal or propagator.[7] Thus if in $\bar{F}(t)$ and $\bar{F}'(t)$ we represent the $\bar{E}$ field to be turned on at t=0 from a zero value for $t<0$, the propagation from $t=-\infty$ to t=0 will result in zero displacement of the electron. Similarly the fields may be turned off at $t=t_2$, but in the evaluation of $\langle x \rangle$ this is not necessary. For example, to calculate v_o one sets $\bar{F}(t) = \bar{E}u(t) + \hat{x}L\delta(t - t_2^-)$ and $\bar{F}'(t) = \bar{E}u(t)$ where $u(t) = 1, t \geq 0$, and $u(t) = 0, t<0$. Because we will use a number of different $\bar{F}(t)$ and $\bar{F}'(t)$, we consider general $\bar{F}$ and $\bar{F}'$ here.

Thus we must evaluate

$$\mathcal{J} = \int\int e^{i\mathcal{F}_0'} \mathcal{D}(\bar{x}(t)) \mathcal{D}(\bar{x}'(t)) \qquad (A-2)$$

where

$$\Phi_o' = \int_{-\infty}^{\infty} dt \left(\tfrac{1}{2} m \dot{\bar{X}}_{(t)}^2 + \bar{F}(t) \cdot \bar{X}(t)\right) - \int_{-\infty}^{\infty} dt \left(\tfrac{1}{2} m \dot{\bar{X}}_{(t)}'^2 + \bar{F}'(t) \cdot \bar{X}'(t)\right)$$

$$+ i \frac{\alpha A}{\sqrt{2}} \int_o^{\infty} d\Omega\, G(\Omega) \int_{-\infty}^{\infty} dt \int_{-\infty}^{t} dt' \left\{ R_\Omega(t-t') \left(\bar{X}'(t) - \bar{X}'(t')\right)^2 \right.$$

$$+ R_\Omega^*(t-t') \left(\bar{X}(t) - \bar{X}(t')\right)^2 - R_\Omega(t-t') \left(\bar{X}(t) - \bar{X}'(t')\right)^2$$

$$\left. - R_\Omega^*(t-t') \left(\bar{X}(t') - \bar{X}'(t)\right)^2 \right\} \qquad (A\text{-}3)$$

First express x, x', F, and F' by their Fourier Transforms:

$$\left.\begin{aligned}
\bar{\xi}_\nu &= \int_{-\infty}^{\infty} \bar{X}(t)\, e^{-i\nu t}\, dt & \bar{X}(t) &= \int_{-\infty}^{\infty} \frac{d\nu}{2\pi}\, \bar{\xi}_\nu\, e^{i\nu t} \\
\bar{\xi}_\nu' &= \int_{-\infty}^{\infty} \bar{X}'(t) e^{-i\nu t}\, dt & \bar{X}'(t) &= \int_{-\infty}^{\infty} \frac{d\nu}{2\pi}\, \bar{\xi}_\nu'\, e^{i\nu t} \\
\bar{f}_\nu &= \int_{-\infty}^{\infty} \bar{F}(t)\, e^{-i\nu t}\, dt & \bar{F}(t) &= \int_{-\infty}^{\infty} \frac{d\nu}{2\pi}\, \bar{f}_\nu\, e^{i\nu t} \\
\bar{f}_\nu' &= \int_{-\infty}^{\infty} \bar{F}'(t)\, e^{-i\nu t}\, dt & \bar{F}'(t) &= \int_{-\infty}^{\infty} \frac{d\nu}{2\pi}\, \bar{f}_\nu'\, e^{i\nu t}
\end{aligned}\right\} \qquad (A\text{-}4)$$

Inserting these in (A-3) gives

$$\iint = \iint e^{i\mathcal{X}}\, \mathcal{D}(\bar{\xi}_\nu)\, \mathcal{D}'(\bar{\xi}_\nu') \qquad (A\text{-}5)$$

where

$$\mathcal{X} = \int_{-\infty}^{\infty} \frac{d\nu}{2\pi} \left(\tfrac{1}{2} m\nu^2 \bar{\xi}_\nu \cdot \bar{\xi}_{-\nu} + \bar{f}_\nu \cdot \bar{\xi}_{-\nu}\right) - \int_{-\infty}^{\infty} \frac{d\nu}{2\pi} \left(\tfrac{1}{2} m\nu^2 \bar{\xi}_\nu' \cdot \bar{\xi}_{-\nu}' + \bar{f}_\nu' \cdot \bar{\xi}_{-\nu}'\right)$$

$$- \frac{4\alpha A}{\sqrt{\beta}} \int_0^\infty G(\Omega)\, d\Omega \int_{-\infty}^{\infty} \frac{d\nu}{2\pi} \Big[\bar{\xi}_\nu' \cdot \bar{\xi}_\nu' \Big(\frac{1}{1-e^{-\beta\Omega}} \frac{\nu}{\Omega(\Omega+\nu+i\epsilon)} - \frac{1}{e^{\beta\Omega}-1} \frac{\nu}{\Omega(\Omega+\nu-i\epsilon)} \Big)$$

$$- \bar{\xi}_\nu \cdot \bar{\xi}_{-\nu} \Big(\frac{1}{1-e^{-\beta\Omega}} \frac{\nu}{\Omega(\Omega+\nu-i\epsilon)} - \frac{1}{e^{\beta\Omega}-1} \frac{\nu}{\Omega(\Omega+\nu+i\epsilon)} \Big)$$

$$- 2i\pi \bar{\xi}_\nu \cdot \bar{\xi}_{-\nu}' \Big(\frac{\delta(\Omega+\nu)}{1-e^{-\beta\Omega}} + \frac{\delta(\Omega-\nu)}{e^{\beta\Omega}-1} \Big) \Big] \qquad (A\text{-}6)$$

We note that since $\bar{x}(t)$, $\bar{x}'(t)$, $\bar{F}(t)$, $\bar{F}'(t)$ are real, $\bar{\xi}_\nu = \bar{\xi}_{-\nu}^*$, $\bar{\xi}_\nu' = \bar{\xi}_{-\nu}'^*$, $\bar{f}_\nu = \bar{f}_{-\nu}^*$, $\bar{f}_\nu' = \bar{f}_{-\nu}'^*$. Thus by changing $\int_{-\infty}^{\infty} d\nu$ to $\int_0^\infty d\nu$ we obtain

$$\iint = \iint e^{iX'}\, \mathcal{D}(\bar{\xi}_\nu)\, \mathcal{D}(\bar{\xi}_\nu^*)\, \mathcal{D}(\bar{\xi}_\nu')\, \mathcal{D}(\bar{\xi}_\nu'^*) \qquad \nu \geq 0 \,, \qquad (A\text{-}7)$$

where

$$X' = \int_0^\infty \frac{d\nu}{2\pi} \Big\{ \big(Z_1(\nu) + Z_2(\nu)\big) \bar{\xi}_\nu \cdot \bar{\xi}_\nu^* - \big(Z_1^*(\nu) + Z_2^*(\nu)\big) \bar{\xi}_\nu' \cdot \bar{\xi}_\nu'^*$$

$$+ \big(Z_2^*(\nu) - Z_2(\nu)\big) \bar{\xi}_\nu \cdot \bar{\xi}_\nu'^* + \big(Z_1^*(\nu) - Z_1(\nu)\big) \bar{\xi}_\nu^* \bar{\xi}_\nu'$$

$$+ \bar{f}_\nu \cdot \bar{\xi}_\nu^* + \bar{f}_\nu^* \cdot \bar{\xi}_\nu - \bar{f}_\nu' \bar{\xi}_\nu'^* - \bar{f}_\nu'^* \bar{\xi}_\nu' \Big\} \qquad (A\text{-}8)$$

and $$Z_1(\nu) = \frac{1}{2}\nu^2 m - \frac{4\alpha A}{\sqrt{\beta}} \int_0^\infty d\Omega\, \frac{G(\Omega)}{1-e^{-\beta\Omega}} \frac{2\nu^2}{\Omega(\Omega^2-\nu^2-i\epsilon)} \qquad (A\text{-}9a)$$

$$Z_2(\nu) = \frac{1}{2} m \nu^2 + \frac{4\alpha A}{\sqrt{\beta}} \int_0^\infty d\Omega\, \frac{G(\Omega)}{e^{\beta\Omega}-1} \frac{2\nu^2}{\Omega(\Omega^2-\nu^2+i\epsilon)} \qquad (A\text{-}9b)$$

These are defined <u>only</u> for $\nu \geq 0$. We are permitted to regard $\bar{\xi}_\nu$ and $\bar{\xi}_\nu^*$ independently for the following reason. The Fourier Transform of $\bar{x}(t)$ has a real part $\bar{a}_\nu$ (even in ν) and an imaginary

part $\bar{b}_\nu$ (odd in ν). To integrate $\bar{x}(t)$ over all possible paths is equivalent to integrating $\bar{a}_\nu$ and $\bar{b}_\nu$ independently over all possible values, but only for those $\nu \geq 0$. And as $\bar{\xi}_\nu$ and $\bar{\xi}^*_\nu$ are simple linear combinations of $\bar{a}_\nu$ and $\bar{b}_\nu$, they are to be integrated independently. Hence, completing the squares in (A-7) we obtain

$$\iint = \exp i \int_0^\infty \frac{d\nu}{2\pi} \left(\frac{\bar{f}^*_\nu (\bar{f}'_\nu - \bar{f}_\nu)}{Z_1(\nu) + Z_2^*(\nu)} + \frac{\bar{f}'_\nu (\bar{f}'^*_\nu - \bar{f}^*_\nu)}{Z_1^*(\nu) + Z_2(\nu)} + \frac{(\bar{f}'_\nu - \bar{f}_\nu)(\bar{f}'^*_\nu - \bar{f}^*_\nu)(Z_2(\nu) - Z_2^*(\nu))}{(Z_1(\nu) + Z_2^*(\nu))(Z_1^*(\nu) + Z_2(\nu))} \right) \quad (A\text{-}10)$$

Letting $Z(\nu) = Z_1(\nu) + Z_2^*(\nu)$, we find

$$Z(\nu) = m\nu^2 + \frac{8\alpha(-A)}{\sqrt{8}} \int_0^\infty d\Omega \, \frac{G(\Omega)}{\Omega} \, \frac{\nu^2}{\Omega^2 - \nu^2 - i\epsilon}, \quad \nu \geq 0 \quad (A\text{-}11)$$

and (A-10) becomes

$$\iint = \exp i \int_0^\infty \frac{d\nu}{2\pi} \left(\frac{f^*_\nu (f'_\nu - f_\nu)}{Z(\nu)} + \frac{f'_\nu (f'^*_\nu - f^*_\nu)}{Z^*(\nu)} - \frac{(f'_\nu - f_\nu)(f'^*_\nu - f^*_\nu)(Z^*(\nu) - Z(\nu))}{Z(\nu) Z^*(\nu)(e^{\beta\nu} - 1)} \right) \quad (A\text{-}12)$$

To convert this result from the frequency to the time domain, we must specify $Z(\nu)$ for negative frequencies, and find an expression for $Y(\nu) = 1/Z(\nu)$. To accomplish this we note that $Z(i\omega)$ is real, and hence that by the Schwartz Reflection Principle, we must have $Z(\nu) = Z^*(-\nu^*)$ for all complex ν which can be reached by analytic continuation of $Z(i\omega)$ off the positive imaginary axis. This condition will be satisfied if we replace ϵ by $\epsilon\nu$ in (A-11),

$$Z(\nu) = m\nu^2 + \frac{8\alpha(-A)}{\sqrt{8}} \int_0^\infty d\Omega \, \frac{G(\Omega)}{\Omega} \frac{\nu^2}{\Omega^2 - \nu^2 - i\epsilon\nu} \qquad (A\text{-}13)$$

for all complex ν. Since we must have Im $(Z(\nu))$ = -Im $(Z(-\nu))$, ν real, and since Im $(Z(\nu)) = \frac{4\alpha(-A)}{\sqrt{8}} G(\nu)$ = -Im $(Z(-\nu))$ for $\nu \geq 0$ and Im $(Z(\nu)) = -\frac{4\alpha(-A)}{\sqrt{8}} G(-\nu)$ = -Im $(Z(-\nu))$ for $\nu \leq 0$, we have $G(0) = 0$. Also we may define $G(\nu) = -G(-\nu)$ consistently for mathematical convenience. Physically this says that if we were to include oscillator potentials with negative frequencies, and hence negative energies $\nu(n + 1/2)$, in our approximate action (12) we would have to change the sign of the coupling to provide for absorption energy.

As written in (A-13), $Z(\nu)$ has no poles in the upper half ν plane. Writing $Z(\nu)$ in an equivalent form as follows

$$Z(\nu) = m(\nu + i\epsilon)^2 + \frac{8\alpha(-A)}{\sqrt{8}} \int_0^\infty d\Omega \, \frac{G(\Omega)}{\Omega} \frac{(\nu + i\epsilon)^2}{\Omega^2 - (\nu + i\epsilon)^2} \quad , \qquad (A\text{-}14)$$

represents a function with neither zeroes nor poles in the upper half plane. If we let $\pi \Gamma(\nu)$ = Im $(Y(\nu))$ = Im $(1/Z(\nu))$, the $\Gamma(\nu)$ is also odd in ν, and using the Kramers-Kronig relations we find

$$\mathrm{Re}\,(Y(\nu)) = P \int_0^\infty \frac{2w\,\Gamma(w)}{w^2 - \nu^2} \, dw \quad . \qquad (A\text{-}15)$$

Combining real and imaginary parts of $Y(\nu)$ we obtain finally

$$Y(\nu) = \int_0^\infty \frac{2w\,\Gamma(w)}{w^2 - \nu^2 - i\epsilon\nu} = 1/Z(\nu) \qquad (A-16)$$

Inserting this expression into (A-12) along with (A-4) and performing $\int_0^\infty d\nu$ gives

$$\mathcal{J} = \int\int e^{i\Phi_0'}\, \mathcal{D}(\bar{x}(t))\, \mathcal{D}(\bar{x}'(t)) =$$

$$\exp \tfrac{1}{2}\Big(\int_{-\infty}^{\infty} dt \int_{-\infty}^{\infty} dt' \Big\{ \bar{F}(t)\cdot\bar{F}'(t) K_\beta(-|t-t'|) +$$

$$+ \bar{F}'(t)\cdot\bar{F}'(t') K_\beta(|t-t'|) - 2\bar{F}(t)\cdot\bar{F}'(t') K_\beta(t-t') \Big\}\Big) \qquad (A-17)$$

where

$$K_\beta(\tau) = \int_0^\infty dw\, \Gamma(w) \left(\frac{e^{iw\tau}}{1-e^{-\beta w}} + \frac{e^{-iw\tau}}{e^{\beta w}-1} \right) \qquad (A-18)$$

It is interesting to note that the form of the result is very similar to the form of the action (A-3).

References for Part II

1 - Feynman, R. P., Phys. Rev. 97, 660 (1955).

2 - Feynman, R. P., Hellwarth, R. W., Iddings, C. K., and Platzman, P. M., Phys. Rev. 127, 1004 (1962). Hereafter referred to as FHIP.

3 - Fröhlich, H., Advances in Physics, edited by N. F. Mott (Taylor & Francis, Ltd., London, 1954), Vol. 3, p. 325.

4 - See this paper for a more thorough justification (p. 1006).

5 - Platzman, P. M., Polarons and Excitons, edited by C. G. Karper and G. D. Whitfield (Oliver & Boyd, Ltd., Edinburgh, 1963), p. 128 ff.

6 - Feynman, R. P., and Vernon, F. L., Annals of Physics 24, 118 (1963).

7 - Feynman, R. P., Rev. Mod. Phys. 20, 367 (1948).

8 - Feynman, R. P., Phys. Rev. 80, 440 (1950).

9 - Fröhlich, H., Theory of Dielectrics, § 18.

10 - Landolt and Bornstein, Zahlenwerte und Funktionen aus Physik, Chemie, Astronomie, Geophysik, Technik, 6. Auflage, II. Band, 6. Teil.

11 - Mead, C. A., J. Appl. Phys. 32, 646 (1961).

12 - Kanter, H., and Feibelman, W. A., J. Appl. Phys. 33, 3580 (1962).